Review Article

Sheikh Tareq Rahman, Kyong Yop Rhee*, and Soo-Jin Park*

Nanostructured multifunctional electrocatalysts for efficient energy conversion systems: Recent perspectives

https://doi.org/10.1515/ntrev-2021-0008
received January 16, 2021; accepted March 11, 2021

Abstract: Electrocatalysts play a significant performance in renewable energy conversion, supporting several sustainable methods for future technologies. Because of the successful fabrication of distinctive oxygen reduction reaction (ORR), oxygen evolution reaction (OER), and hydrogen evolution reaction (HER) electrocatalysts, bifunctional ORR/OER and HER/OER electrocatalysts have become a hot area of contemporary research. ORR, OER, and HER have gained considerable attention because of their strong performance in different energy conversion and storage devices, including water-splitting devices, fuel cells, and metal–air rechargeable batteries. Therefore, the development of effective nanostructured multifunctional electrocatalysts for ORR, OER, and HER is necessary; and there is a demand for their industrialization for sustainable energy technology. In this review, details of current improvements in multifunctional catalysts for ORR/OER as well as HER/OER are presented, focusing on insight into the theoretical considerations of these reactions through investigation and estimation of different multifunctional catalysts. By analyzing the universal principles for various electrochemical reactions, we report a systematic scheme to clarify the recent trends in catalyzing these reactions over various types of nanostructure catalysts. The relevant reaction pathways and the related activity details for these reactions in the current literature are also included. Overall, the current demands and future outlines for improving the prospects of multifunctional electrocatalysts are discussed.

Keywords: oxygen reduction reaction, oxygen evolution reaction, hydrogen evolution reaction, nanomaterials, electrocatalysts

*** Corresponding author: Kyong Yop Rhee,** Department of Mechanical Engineering, College of Engineering, Kyung Hee University, Yongin, 17104, Republic of Korea, e-mail: rheeky@khu.ac.kr, tel: +82-31-201-2565; fax: +82-32-202-6693
*** Corresponding author: Soo-Jin Park,** Department of Chemistry, Inha University, 100 Inharo, Incheon 22212, Republic of Korea, e-mail: sjpark@inha.ac.kr, tel: +82-32-876-7234; fax: +82-32-860-8438
Sheikh Tareq Rahman: Department of Chemistry, Inha University, 100 Inharo, Incheon 22212, Republic of Korea, e-mail: rahman19@inha.edu

1 Introduction

The necessity of sustainable progress for human society and awareness of serious environmental pollution have accelerated the progression from nonrenewable fossil fuels to green alternative energies (such as tidal, solar, and wind power) [1]. Renewable tidal energy sources and their conversions are vital for sustainable advancement and ecological continuity [2]. However, traditional renewable power sources have only gained limited widespread acceptance in the global energy sector because of their instability due to time and place factors [3]. Therefore, it is essential to improve innovative sustainable energy conversion and high-capacity depository electronic components such as water-splitting devices, rechargeable fuel cells, and metal–air batteries [4–6]. Moreover, efficient nanostructured electrocatalysts are desired to reduce the static kinetics and extensive overpotential of the oxygen reduction reaction (ORR), oxygen evolution reaction (OER), and hydrogen evolution reaction (HER) to improve green energy in the restoration of traditional fossil fuel energy on account of the serious environmental pollution [7]. Although the Pt noble metal outlasts the high-effective activities for the ORR and HER, the cost and low resistance of these platinum group metals limit their wide-scale adoption [8–11]. Hence, a promising opportunity would be the ability to modify the molecules in the surroundings (*e.g.*, carbon dioxide, water, and air) into beneficial chemicals (*e.g.*, ammonia, oxygen, hydrogen, and hydrocarbons) to set up a “zero-emission”

sustainable energy transformation process depending on earth-abundant nonnoble metals [12–14].

In recent years, several useful energy conversion processes have been developed; the foremost is the nonnoble metal catalysts as replacements for Pt- and Ru-type catalysts [15–17]. These systems, including water electrolysis, fuel cells, and rechargeable metal–air batteries, depend on a series of electrochemical reactions along with HER, OER, and ORR, which have already been extensively reported [18–21]. Although these advanced electrochemical reactions are continually restricted by sluggish kinetics, they lead to a high overpotential as well as a low full-circle ability [22–24]. It is important to focus on the improving effective electrocatalysts for OER, ORR, and HER to enhance the reaction rates. Recently, several electrocatalysts have been reported for ORR/OER and HER/OER due to a decline in the costs of synthesis and devices. Nevertheless, because the hydrogen and oxygen evolution reactions take place in dissimilar conditions, only a few catalysts can act as bifunctional and trifunctional electrocatalysts for both reactions [25,26]. However, the best ORR catalyst generally has low OER performance, whereas the best OER catalyst has low HER catalytic activity [27]. Meanwhile, their extensive industrial application is hindered by the high cost of noble metal-type electrocatalysts and limited resources. Recently, transition-metal-based catalysts and perovskites have been reported as the low-cost electrocatalysts for metal–air cells [28–32]. Co-, Ni-, and Fe-type sulfides, phosphides, and hydroxides have presented excellent electrocatalytic performance in water splitting [33–36]. Interestingly, electrochemical water splitting supplies a promising technique to realize sustainable high-purity hydrogen production [37]. Moreover, N-doped carbon nanomaterials are a favorable alternative for OER/HER/ORR multifunctional electrocatalysts [38–40]. In electrolysis reactions, HER and OER store energy; whereas in the fuel-cell approach, the ORR is responsible for energy conversion [22,41] (Figure 1).

In this review, we describe an overview of electrocatalysts, summarize recent progress, and discuss the emerging functions for ORR, OER, and HER in sustainable energy technologies. Due to the breadth of this topic, particular attention has been paid to inexpensive heterogeneous inorganic metal electrocatalysts such as metal sulfides, metal selenides, metal carbides, metal nitrides, metal phosphides, and heteroatom-doped nanocarbons for which promising alternatives are available for earth-abundant electrocatalysts including ORR, OER, and HER. Furthermore, we summarize the synthesis, activity, and durability of distinct efficient electrocatalysts, including Co-based single atom and composites, utilized as bifunctional electrocatalysts of OER/HER or ORR/OER, and N-doped graphene nanosheets as upgraded multifunctional metal-free catalysts for the ORR, OER, and HER. Noble metal-containing catalysts are not discussed in detail here. We give an overview of current developments in the high-performance earth-abundant inorganic electrocatalysts, focusing our discussion on promising types of materials. We cannot assure that this review covers all work related to this topic, because of the significant progress and increasing rate of publication in this research field; instead, we focus on prevailing themes and major improvements that have determined the primary directions for the upcoming research.

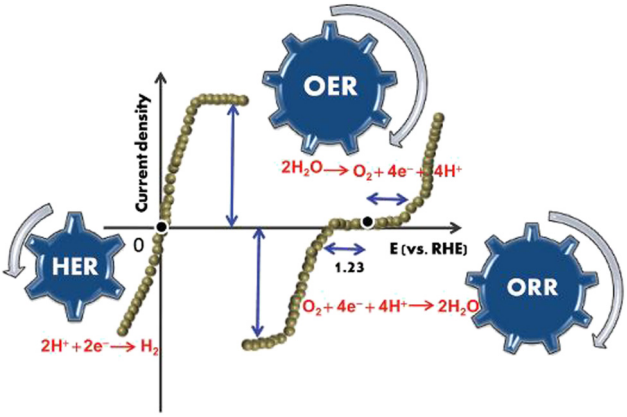

Figure 1: Schematic illustration of electrochemical reactions associated with water splitting. Reprinted from ref. [22]; copyright (2018), Royal Society of Chemistry.

2 Integral features of electrochemical reactions

2.1 Reaction technique for the ORR

The electrochemical ORR is a crucial cathodic electrode reaction because of its use in rechargeable energy equipment, including hydrogen fuel batteries and metal–air cells [42,43]. The ORR process links several coupled proton and electron exchange steps to molecular oxygen evolution at the cathode. The ORR method usually occurs through two different pathways in both alkaline and acidic electrolyte solutions [44–46]. The first pathway is the four-electron, one-step route, and the second one is the less efficient two-electron, two-step route.

The routes in alkaline conditions are demonstrated as follows:

(1) A straightforward four-electron ORR:

$$O_2 + 2H_2O + 4e^- = 4OH^- \quad (E^o = 0.41\ V) \qquad (1)$$

(2) The preferred two-electron route connects reduction to the production of HO_2^- medium:

$$O_2 + H_2O + 2e^- = HO_2^- + OH^- \quad (E^o = 0.065\ V) \qquad (2)$$

$$HO_2^- + H_2O + 2e^- = 3OH^- \quad (E^o = 0.0867\ V) \qquad (3)$$

The ORR routes in acidic conditions are as follows:

(1) A straightforward four-electron ORR:

$$O_2 + 4H^+ + 4e^- = 2H_2O \quad (E^o = 1.229\ V) \qquad (4)$$

(2) A two-electron route containing oxygen reduction by the production of H_2O_2 medium:

$$O_2 + 2H^+ + 2e^- = H_2O_2 \quad (E^o = 0.7\ V) \qquad (5)$$

$$H_2O_2 + 2H^+ + 2e^- = 2H_2O \quad (E^o = 1.76\ V) \qquad (6)$$

Selectivity against the four-electron oxygen reduction system depends on increasing the electrocatalyst's ability to increase the reaction rate. Typically, the ORR comprises either a four-electron exchange to decrease oxygen, which is ideal in certain types of cells, or a two-electron route required for the formation of H_2O_2. Furthermore, from the above standard thermodynamic potential analysis, the ORR system has lower potential and better kinetics in basic conditions than in acidic ones [22,47,48].

Based on several possible pathways, many groups searched for the rate-determining step (RDS). Usually, ORR kinetics on metal catalysts are primarily restricted by the following three steps: (1) the first electron exchange of the ORR, (2) the hydration of oxygen, and (3) the desorption of the intermediates. Many researchers have determined that the first electron exchange involves the RDS of the ORR [49–53]. For instance, by using reaction center models and self-consistent *ab initio* calculations, Anderson and Albu [54] reported the activation energies of the basic steps of the ORR. They noticed that the first electron transfer step had the largest activation energy on Pt catalysts, and proton exchange occurred in the RDS. Other groups came to similar conclusions by applying different approaches to the investigation of the first electron exchange step [55]. However, Yeh *et al.* demonstrated a different view on the order of the electron and proton exchange [56]. They noticed that the first electron transfer preceded the protonation of the adsorbed O_2 molecules; specifically, the protons, associated with the adsorbed O_2 molecules were in the form of H_3O^+. The ORR process may differ with the varying nanostructures of the electrocatalysts. Generally, not only the O_2 adsorption but also the O^{2-} surface interactions influence the ORR routes [45,57]. In the theoretical ORR volcano plot, electrocatalytic activity *vs* ΔE_o was constructed (Figure 2a), which is dependent on the free energies of the substances described above on different metal surfaces [21,44,48]. Although Pt exhibits the best ORR electrocatalytic activity in theory, it does not appear at the "summit of the volcano" (Figure 2a); however, using different 3d/4d transition metals has been recognized as a better idea to develop its efficiency [58,59].

2.2 Reaction technique for the OER

The OER is the basis for all systems using inversion processes along with the ORR and/or HER [60–65]. The OER that occurs in the anodic electrochemical reaction in water splitting and several kinds of batteries is a more

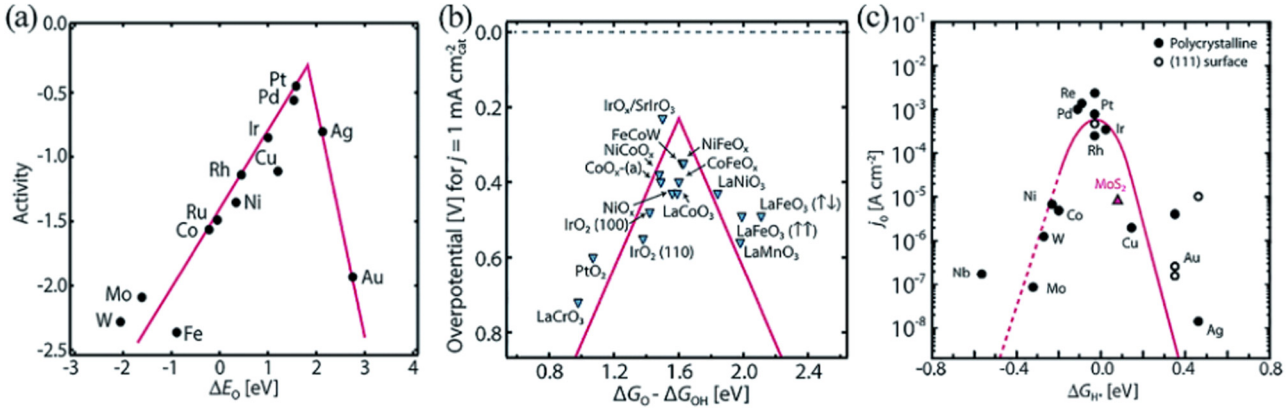

Figure 2: (a) Metals volcano plot for the ORR system redrawn from [21], copyright 2017, WILEY-VCH; (b) Metal oxides volcano plot for OER system redrawn from [44], copyright 2017, American Association for the Advancement of Science; (c) metals volcano plot for the HER system redrawn from [44], copyright 2017, American Association for the Advancement of Science.

complex mechanism than that of the ORR. Experimental analysis has shown that Pt is not ideal for the OER, which has been demonstrated by a particular ORR on Pt [44]. The reason Pt is not ideal is that microscopic reversibility occurs in this method, ensuring that it is close to equilibrium. While a high overpotential is applied to run the reverse reactions, the conditions for the electrochemical reactions can be extremely different for each route [66,67]. In the complex OER system, oxygen evolves from a metal oxide surface at a high potential, and the reaction technique varies for those oxides with various surface frameworks [67,68]. Volcano plots have been designed for a wide range of metal oxide surfaces with $\Delta G_O - \Delta G_{OH}$ on the *x* axis (Figure 2b) for the OER. In the OER, equation (7) is the half-reaction of water splitting. The cathodic and anodic reactions for water splitting are dissimilar under acidic (equations (8) and (9)) and basic media (equations (15) and (16)). Several groups have suggested viable pathways for the OER at the anodic electrode either in acidic (equations (10)–(14)) or in alkaline solutions (equations (17)–(21)), and there are some similarities and differences. Most of the techniques produce similar intermediates, including metal hydroxides and metal oxides (MOs), while the major differences are most likely how oxygen is formed during the reaction. Chen *et al.* reported two different routes for the production of oxygen from MO intermediates (Figure 3) [67]. The first one is shown as a green pathway in Figure 3, in which 2MO forms O_2(g) (equation (12)). The second one is associated with the formation of an MOOH intermediate (equations (13) and (20)), which consequently dissolves to O_2(g) (black lines in Figure 3; equations (14) and (21)).

$$2H_2O \rightarrow 2H_2 + O_2 \tag{7}$$

In acidic media, the following reactions occur.

Cathode reaction:

$$4H^+ + 4e^- \rightarrow 2H_2 \quad E_c^o = 0\,V \tag{8}$$

Anode reaction:

$$2H_2O(l) \rightarrow O_2(g) + 4H^+ + 4e^- \quad E_a^o = 1.23\,V \tag{9}$$

The expected technique in acidic media is the following:

$$M + H_2O(l) \rightarrow MOH + H^+ + e^- \tag{10}$$

$$MOH + OH^-(l) \rightarrow MO + H_2O(l) + e^- \tag{11}$$

$$2MO \rightarrow 2M + O_2(g) \tag{12}$$

$$MO + H_2O(l) \rightarrow MOOH + H^+ + e^- \tag{13}$$

$$MOOH + H_2O(l) \rightarrow M + O_2(g) + H^+ + e^- \tag{14}$$

In alkaline media, the following reactions occur.

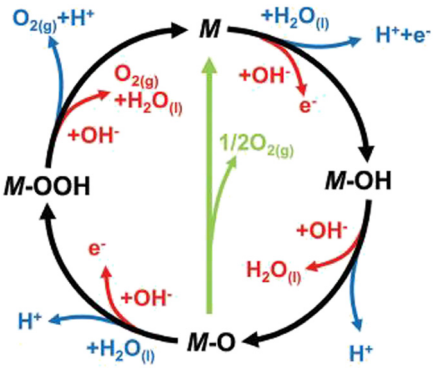

Figure 3: The OER technique in acidic (blue line) and basic (red line) solutions. The black line shows that the OER connects the production of a peroxide (M–OOH) intermediate (black line) with the formation of oxygen, while another way to form oxygen is the reaction of two adjoining oxo (M–O) intermediates (green). Redrawn from [67]; copyright 2017, Royal Society of Chemistry.

Cathode reaction:

$$2H_2O(l) + 4e^- \rightarrow 2H_2(g) + 4OH^- \quad E_c^o = -0.83\ V \tag{15}$$

Anode reaction:

$$4OH^- \rightarrow 2H_2 + H_2O(l) + 4e^- \quad E_a^o = -0.40\ V \tag{16}$$

The expected technique in alkaline media is as follows:

$$M + OH^-(l) \rightarrow MOH \tag{17}$$

$$MOH + OH^-(l) \rightarrow MO + H_2O(l) \tag{18}$$

$$2MO \rightarrow 2M + O_2(g) \tag{19}$$

$$MO + OH^- \rightarrow MOOH + e^- \tag{20}$$

$$MOOH + OH^- \rightarrow M + O_2(g) + H_2O(l) \tag{21}$$

2.3 Electrochemistry of HER

HER is a two-electron exchange cathodic reaction that occurs during electrochemical water splitting [18,69]. The pH of the electrolyte is the most essential factor determining HER rate. HER can be carried out chemically by different pathways in various electrolytes, which are illustrated as follows [70,71]:

In acidic conditions,

(1) An adsorbed hydrogen atom (H_{ads}) is formed by an electron and a proton on the catalyst surface, which is known as Volmer step:

$$H_3O^+ + e^- \rightarrow H_{ads} + H_2O \tag{22}$$

(2) A hydrogen molecule is formed by H_{ads}, which gains a proton and electron, and is known as Heyrovsky step:

$$H_3O^+ + e^- + H_{ads} \rightarrow H_2 + H_2O \quad (23)$$

(3) Or, by Tafel step, a hydrogen molecule is formed by two adsorbed hydrogen atoms.

$$H_{ads} + H_{ads} \rightarrow H_2 \quad (24)$$

In the basic conditions, HER progresses by a particular Volmer step and a subsequent Heyrovsky step.

(1) Because of the H^+ deficiency, H_2O interacts with an electron to produce OH^- and H_{ads} on the electrocatalyst.

$$H_2O + e^- \rightarrow OH^- + H_{ads} \quad (25)$$

(2) The H_{ads} couples with an electron and water to form a hydrogen molecule.

$$H_{ads} + H_2O + e^- \rightarrow OH^- + H_2 \quad (26)$$

(3) A hydrogen molecule is formed by two adsorbed hydrogen atoms, which is similar to the Tafel step in acidic conditions.

$$H_{ads} + H_{ads} \rightarrow H_2 \quad (27)$$

From the above HERs, it can be observed that the Volmer reaction in the basic electrolyte condition demands breakage of the H–O–H bond before adsorbing H_{ads}, which is further challenging than the reduction of H_3O^+ in an acidic electrolyte solution. Thus, an acidic media is more favorable than alkaline media for HER.

The hydrogen adsorption free energy (ΔG_H) on Pt is almost zero (Figure 2c) [44,71,72], which was experimentally measured by density functional theory (DFT) calculations. In the volcano plots in Figure 2a–c, it is worth noting that Co performed better in ORR and HER activities than the similar transition metals Fe and Ni. At the same time, the theoretical OER activity of NiO_x was lower than that of CoO_x. In this review, specific consideration was paid to the Co-based catalytic approach to ORR/OER/HER and promising approaches for increasing this activity.

3 Evaluation of bifunctional electrocatalysts

3.1 Bifunctional electrocatalysts for the ORR and OER

Mn-, Fe-, Co-, and Ni-type nonnoble metal oxides are used as catalysts for the ORR and OER in basic conditions, due to their electrocatalytic activity and extensive stability in oxidative conditions [73–79]. Currently, the ORR/OER features of some emerging nonnoble metal oxides in basic solution exceed the activities of updated Ru-, Ir-, and Pt-based catalysts [80–84]. Manthiram's group has recently reported the ORR and OER characteristics of lithium cobalt oxide ($LiCoO_2$) in basic conditions [85]. The high efficiency of $Li_{1-X}CoO_2$ was fundamentally connected to the production of combined valence Co^{3+}/Co^{4+} ions, which strongly increased its catalytic activity [86]. Therefore, conscious design of the surface active sites, which determine the phase and structure, is an efficient way of producing more inexpensive and effective transition metal oxide nanocatalysts.

3.1.1 Spinel-based oxides

Transition metal oxides (TMOs) along with a spinel composition have gained spotlight owing to their particular and strong elctrocatalytic abilities for the ORR and OER in basic conditions. Co_3O_4, $NiCo_2O_4$, $CoMn_2O_4$, and $LiCo_2O_4$ are the most reported metal-doped spinel-based catalysts for both the ORR and OER [85,87,88]. These types of catalysts have been synthesized with advanced nanochain structures [89] and 3D architectures [80], resulting in good mass-transport features and increased activity for ORR/OER. However, poor catalytic activity is the disadvantage of spinel-type catalysts for ORR/OER catalysis due to their low electronic forces as well as low oxygen adsorption on the surface of the spinel oxides [80,81,90]. Therefore, many approaches have been taken to develop an improved synthetic process for spinel oxides. Carbon and its derivatives have been analyzed as highly conductive supports for catalysts owing to their high surface area, excellent electronic forces, favorable useful characteristics and superior material durability [90–92]. Co-based carbon phosphides (CoPs) are also an effective approach for increasing the electropotentiality and reliability of the OER/ORR catalysts. Moreover, Song *et al.* [93] reported cobalt-based phosphides with defective carbon (CoP–DC) nanohydrids as multifunctional electrocatalysts which has enhanced ORR performance on the DC and subsequently increased the OER performance on the CoP. This group concurrently investigated their interfacial charge distribution characteristics. The interfacial charge distribution of the electrons was condensed on the DC surface by integrating multiple atomic accelerator-based X-ray adsorption properties with DFT calculations, while the holes on the CoP surface were assembled by active interfacial coupling, which concurrently promoted the ORR and OER with notable multifunctional performance

(Figure 4a and b). Furthermore, Manthiram's group [94] proposed significant multifunctional activity for the OER and ORR over CoP nanoparticles hybrids on an N-, an S-, and a P-doped graphene matrix (CoP@mNSP–C), whereas the energy gap value (ΔE) of CoP@mNSP–C was much lower (0.74 V) than those of the other cobalt-associated electrocatalysts. Interestingly, the CoP nanoparticles were transferred to the metal (Co) oxide *in situ* during the reactions, which decreased the anodic current utilized by the carbon. The support provided by the graphene material maintains the primary electrocatalytic characteristics of the hybrid electrocatalyst. Jiang's group [95] reported an innovative $CoMnP_4$ nanoparticles as a bimetallic phosphide catalyst along with P, N co-doped carbon tiers (CMP@PNC) over a distance-restriction phosphorization approach, as illustrated in Figure 4c. In this situation, the P and N mixed-doped carbon beds enhanced the enclosed bimetallic phosphide by providing a large number of catalytic sites, thereby permitting it to achieve remarkable electrocatalytic performance.

Liang *et al.* [96] studied a bifunctional catalyst for ORR and OER, which was fabricated in a two-step process, producing a Co_3O_4/N-rGO reduced graphene oxide nanomaterial [58]. They enhanced its ORR and OER performance by mixing Co_3O_4 and N-doped graphene because their cooperative chemical coupling can increase the catalytic efficiency of ORR and OER. Other hybrid materials including a Co_3O_4/N-type carbon nanoweb [83], $MnCo_2O_4$/carbon [92], and $FeCo_2O_4$/hollow carbon spheres [81] have been synthesized as superior multifunctional catalysts. Moreover, Chen *et al.* observed that considering the structure and function is a favorable approach for developing the catalytic stability of spinel-based oxides [97]. They have experimentally synthesized ultra–small $Co_xMn_{3-x}O_4$ by an easy solution-type oxidation precipitation in air and an inclusion-crystallization method in soft conditions (Figure 5a). Interestingly, when connected with graphene, the nanocrystalline cubic spinel combined electrocatalyst has naturally enhanced ORR and OER characteristics competed with Pt/C catalysts (Figure 5b). Remarkably, due to its outstanding multifunctional ORR/OER performance and strength, the cubic spinel mixed electrocatalyst revealed surprising recharge performance at a flat discharge/charge rate and over potential (Figure 5c).

3.1.2 Perovskite-type catalysts

Perovskites are often used as multifunctional electrocatalysts for the ORR and OER in the practical application of several energy conversions as well as storage devices,

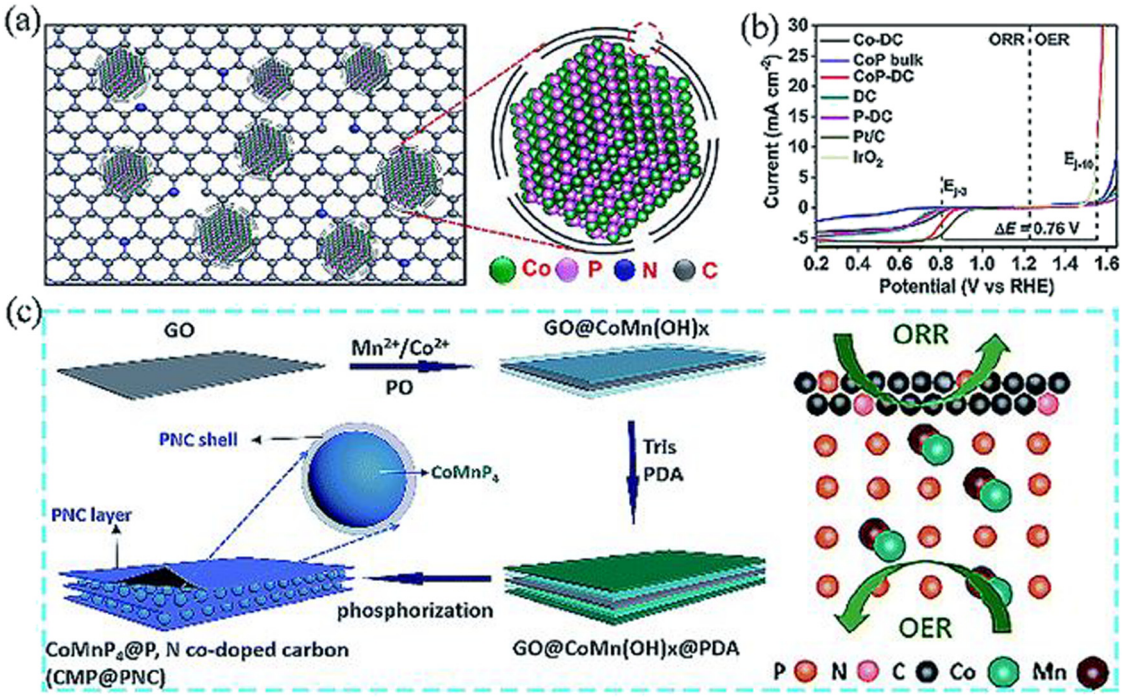

Figure 4: (a) Schematic illustration of the CoP–DC framework (b) The complete linear sweep voltammetry bends of the CoP–DC model over the entire ORR and OER areas in basic solution (0.1 M KOH). Redrawn from ref. [93], copyright 2018, WILEY-VCH. (c) Synthesis of the enclosed bimetallic phosphide-type CMP@PNC catalyst, and a diagram of the ORR and OER-sites. Redrawn from [95], copyright 2018, Royal Society of Chemistry.

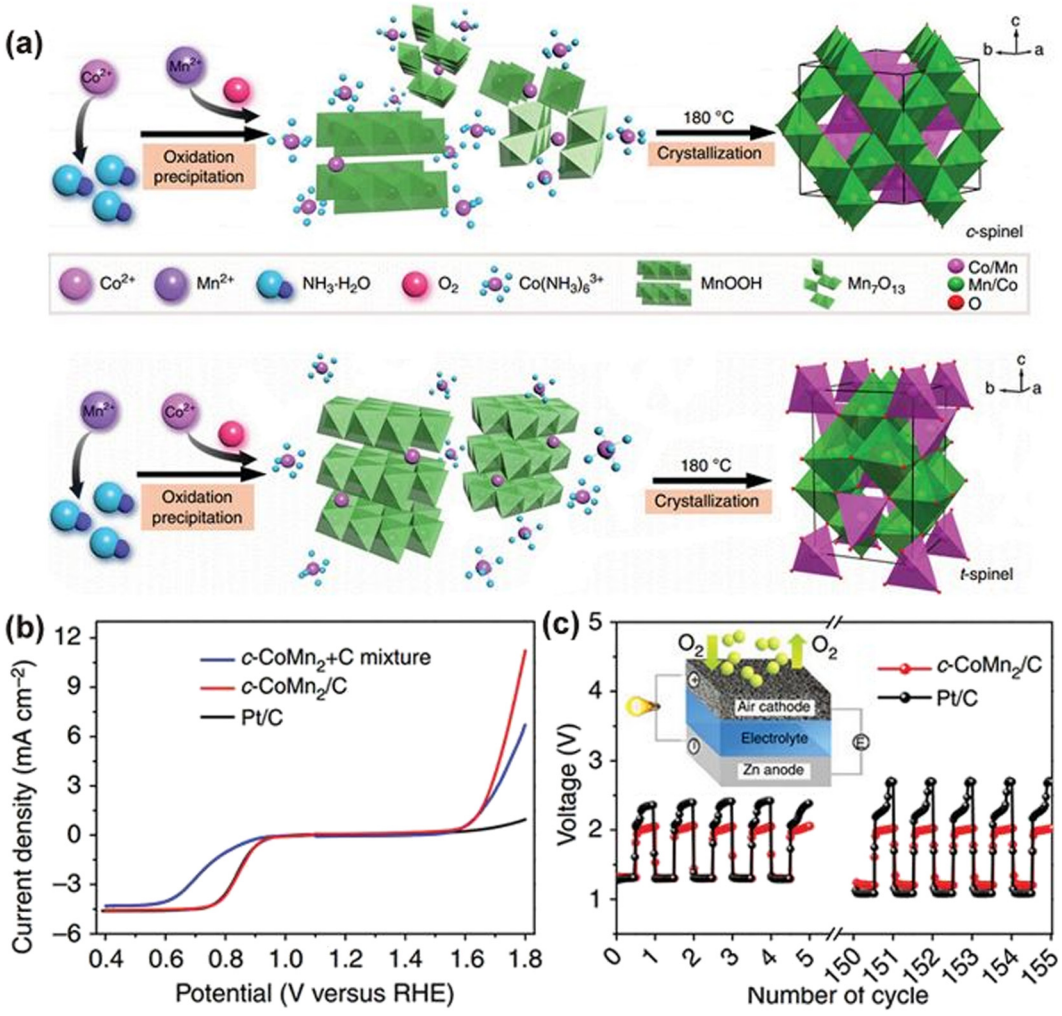

Figure 5: (a) Diagram of the fabrication of cubic (I) and tetragonal (II) spinel conditions in two phases: oxidation precipitation step and crystallization step respectively. (b) The ORR and OER performances of mixed *c* –$CoMn_2$/C, *c* –$CoMn_2$/C hybrid and Pt/C catalysts in basic solution (0.1 M KOH). (c) Catalytic activities of rechargeable Zn–air batteries applying *c* –$CoMn_2$/C, and Pt/C as cathodic ORR electrocatalysts at a 10 mA cm^{-2} looping rate and a period of 400 s per loop. The inset illustrates the framework of an amassed rechargeable Zn–air battery. Redrawn from [97], copyright 2015, Nature Publishing Group.

including fuel cells [98,99] and metal–air batteries [100,101]. Thus, several groups have been studying the possible pathways of perovskites electrocatalysis over a long period. Compared with some nonnoble metal oxides, perovskite-based oxides have shown various exclusive characteristics, including tunability of the electronic framework and cations, ideal textures for oxygen vacancy, and high oxygen transport kinetics [84,102–104]. Many researchers have reported that the exchange of metal ions and the arrangement of oxygen mobility can effectually increase the catalytic activity of ORR/OER [105–107]. Cho *et al.* attempted to assemble a series of highly active chemicals that depend on $Ba_{0.5}Sr_{0.5}Co_{0.8}Fe_{0.2}O_{3-\delta}$ as ORR/OER electrocatalysts [84,108,109]. In one of their studies, a La-doped $Ba_{0.5}Sr_{0.5}Co_{0.8}Fe_{0.2}O_{3-\delta}$ nano-framework catalyst was synthesized as an efficient multifunctional catalyst for both the ORR and OER.

The oxide electrode mixtures exist of 80 wt% oxide elements and 20 wt% KB, and Pt/C 20% consists of 20 wt% Pt and 80 wt% Vulcan XC-72(E-tek). The all-oxide electrode compounds have 0.64 mg_{ox} cm^{-2} disks, 0.16 mg_{KB} cm^{-2} disks, 0.35 mg_{Nafion} cm^{-2} disks, while the Pt/C 20% electrode has a 0.16 mg_{Pt} cm^{-2} disk, a 0.64 mg_{XC-72} cm^{-2} disk, and a 0.35 mg_{Nafion} cm^{-2} disk. Reproduced from [84], copyright 2015, WILEY-VCH.

Although the amount of the single $LaCoO_3$ component was comparatively low, its inclusion enhanced ORR and OER catalysts when competed with $Ba_{0.5}Sr_{0.5}Co_{0.8}Fe_{0.2}O_{3-\delta}$. However, Hjalmarsson's group [110] reported that the production of secondary layers on the surfaces of

perovskite oxides could restrict their electrocatalytic performance. In contrast, Jung *et al.* [84] took the unique approach of modifying the surface chemistry and morphology by a heating process carried out in oxygen for increasing amounts of time. In addition, the heating method promotes the generation of the complete cubic perovskite texture and clears away the ultrathin surface bed spinel stage between the amorphous level (=30 nm) and cubic perovskite particle amount, which is involved in the development of the electrocatalytic activity of $Ba_{0.5}Sr_{0.5}Co_{0.8}Fe_{0.2}O_{3-\delta}$ catalyst (Figure 6a). These perovskite catalysts exhibit highly adaptable ORR/OER activities compared with pristine $Ba_{0.5}Sr_{0.5}Co_{0.8}Fe_{0.2}O_{3-\delta}$ and activities similar to those of noble-metal catalysts for ORR/OER (Figure 6b and c). Therefore, the electrocatalytic properties of perovskite oxides can be enhanced through the exchange of metal ions and the arrangement of oxygen vacancies. Addition of other elements into the

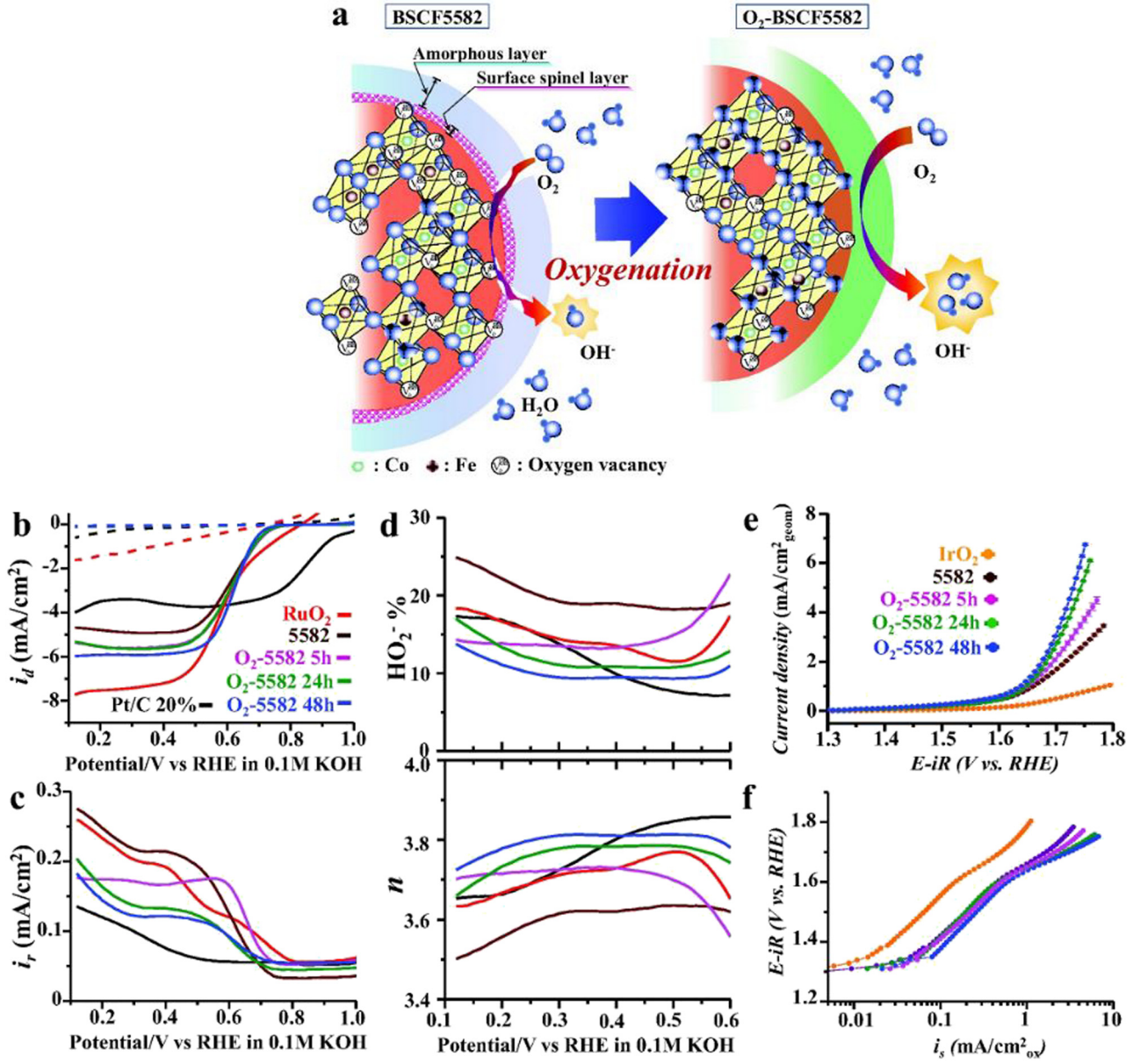

Figure 6: (a) Demonstration of the impact of heat analysis in oxygen on BSCF5582. (b) The ORR performances of BSCF5582 and O_2-BSCF5582 in basic condition (0.1 M KOH) under saturated oxygen gas (solid lines) and argon gas (dotted lines). (c) Ring currents (voltammograms) of the ORR and the resolved (d) peroxide percentage (HO_2-%) and electron-transfer number (*n*) applying rotating ring-disc electrodes (RRDEs) at 1600 rpm and a scan rate of 10 mV s^{-1} in same conditions. (e) The OER performances of BSCF5582 and O_2-BSCF5582 in same conditions. (f) Tafel plot of the OER-specific performances of BSCF5582 and O_2-BSCF5582.

perovskite oxide framework can enhance its performance (for instance, $LaNiO_3$/N-type CNTs [111], $La_{0.8}Sr_{0.2}MnO_{3-\delta}/Ba_{0.5}Sr_{0.5}Co_{0.8}Fe_{0.2}O_{3-\delta}$ [102], $La_{0.8}Sr_{0.2}MnO_3$/carbon [82], and $Ba_{0.5}Sr_{0.5}Co_{0.8}Fe_{0.2}O_{3-\delta}$/carbon [103]). These hybrid electrocatalysts exhibit high ORR/OER properties because of the collective element coupling impacts.

3.1.3 Metal-free electrocatalysts

Metal-based catalysts have some drawbacks, including high cost, low conductivity, and destructive environmental effects [112–114]. Therefore, there is a push to synthesize metal-free ORR and OER catalysts that have high activity, low expense, and excellent durability and that are environmental friendly towards these reactions [112,115–117]. Heteroatom-doped carbon-based catalysts and their hybrids represent two initial types of metal-free electrocatalysts for ORR and OER in basic conditions. Their distinctly large surface areas, flexible nanostructures, and particular electronic morphologies offer high electrocatalytic activity. It has been reported that the combination of N, S, and P atoms with graphene can effectively adjunct the electronic framework of the enclosing carbon atoms and regulate the regional charge frequency distribution, which resulted in the improvement of the electrocatalytic efficiency [112,116,117]. Nevertheless, the largest active sites of different atom with carbon synthesized by classical chemical loading were not allocated on the surface of the catalysts, which resulted in poor catalytic performance. Therefore, Tian *et al.* [118] fabricated a core-shell electrocatalyst composed of pristine carbon nanotubes (CNTs) in the center and N-doped carbon beds as the framework; these catalyst has outstanding ORR/OER performance. They reported that the surface N/C ratios were mainly based on the period of crystalline progress and were adjusted in from 0.0238 to 0.145. The N-atom enhancement on the surface of the catalysts clearly revealed the active sites which were responsible for its ORR/OER efficiency. Moreover, Dia's group reported that an innovative 3D N and P mixed-type mesoporous carbon foam (NP-MCF) enhances ORR and OER performance because of its high surface area of 1,663 $m^2 g^{-1}$ [119]. This catalyst was synthesized by a straightforward pyrolysis of polyaniline (PANi) aerogels template-free process in the existence of phytic acid at 1,000°C (Figure 7a). That group examined the suitability of this NP–MCF for Zn–air cells' air electrode; it exhibited a large open-circuit current (1.48 V), high efficiency (735 mA h g^{-1}), and superior peak energy frequency (55 mW cm^{-2}). Interestingly, di-electrode renewable Zn–air cells along with NP–MCF as the multifunctional electrocatalysts exhibit high efficiency better than that of combined Pt/C and RuO_2 electrocatalyst (Figure 7b). Although a decline in efficiency was noticed for the dielectrode renewable Zn–air cell during a comprehensive circuit analysis, the characteristics of the NP–MCF-type cell were generally enhanced by fabrication of an upgraded three-electrode battery (Figure 7c). They studied the electrocatalytic efficiency of the two air electrodes (ORR or OER), which were mostly based on mass doping. The NP–MCF-type battery demonstrated outstanding activity with high stability and comprehensive discharge/charge loops, similar to or even greater than those of the combination Pt/C and RuO_2 or only Pt/C elctrocatalysts (Figure 7d and e).

The deliberate creation of 3D adaptable nanostructures with balanced frameworks is a favorable approach for enhancing catalytic features. For instance, Ma *et al.* [120] revealed P-doped carbon nitride nanoflowers developed *in situ* on carbon–fiber paper (PCN/CFP) as adjustable, coverless oxygen electrodes. Although the performance of pristine CFP is imperceptible, PCN/CFP showed a starting energy of 0.94 V *vs* RHE and a 0.67 V half-circle power *vs* RHE, similar to those of a Pt-type electrocatalyst (starting energy = 0.99 V, half-circle energy = 0.8 V). The PCN/CFP also managed a beginning energy of 1.53 V in the OER, and lower Tafel slope (61.6 mV dec^{-1}) than that of CN/CFP, allowing easy electron exchange and affording a high surface area which was catalytically active, while the P-doped carbon nitride supplies high catalytic efficiency due to the dual action of N and P.

3.2 Bifunctional electrochemical activities for HER and OER

HER and OER compose the two half-cell reactions of water splitting, which are essential for its overall efficiency. However, developing uniform catalysts that can initiate both reactions with the lowest possible overpotentials, and make the water-splitting method less energy-intensive is a tough challenge. Pt-based catalysts for HER reduced the OER activity, while the Ir- and Ru-type OER catalysts have low HER performance [121–123]. For that reason, many cheap and earth-sufficient non-noble metals have been improved in current years as hydrogen and oxygen evolution catalysts with high potential catalytic efficiency. Basic water splitting has become the favored method for mass production of H_2, but acidic water splitting requires unique and overpriced

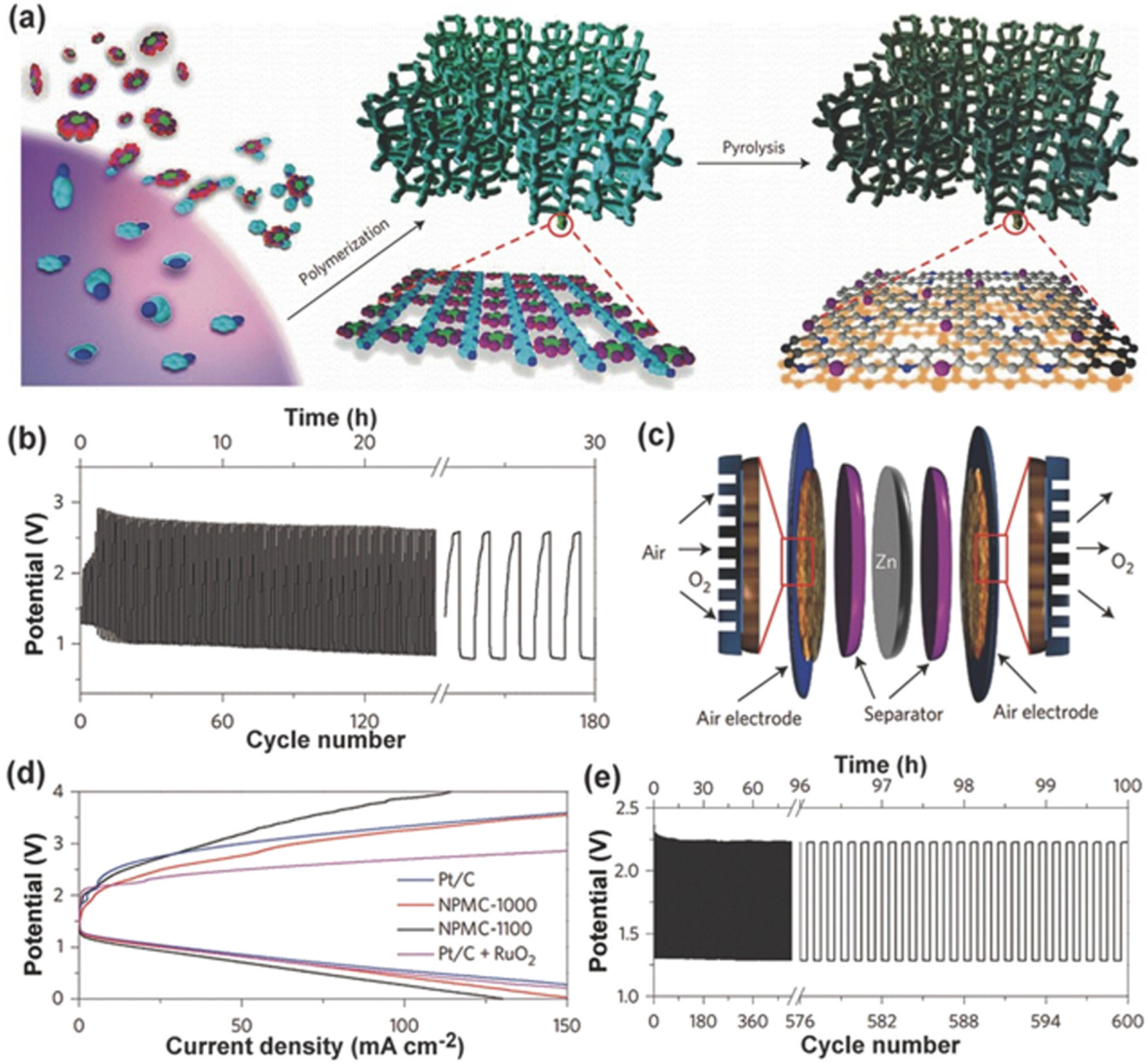

Figure 7: (a) Synthesis of NP–MC foams. (b) The discharge/charge series loops of dielectrode renewable Zn–air cells at a 2 mA cm^{-2} current density depend on the NP–MC-1000 air electrode. (c) Diagram of a tri-electrode Zn–air cell. The extended sections form the porous frameworks of the air electrodes, promoting gas transfer. (d) Charge and discharge polarization loops of trielectrode Zn–air batteries utilizing NP–MC-1000, NP–MC-1100, or an industrial Pt/C electrocatalyst. (e) Series loops (charging/discharging) utilizing NP–MC-1000 for the air electrodes; whereas that catalyst was used 0.5 mg cm^{-2} for ORR as well as 1.5 mg cm^{-2} for OER, and current density was 2 mA cm^{-2}. Redrawn from [119], copyright 2015, Nature Publishing Group.

OER catalysts for using in acidic media [124]. Therefore, various strategies have been developed to fabricate catalysts with strong HER [125] and OER [126] efficiency: (1) combining the most active electrocatalysts in a particular hierarchical framework to enhance the co-active electrochemistry for the entire water-splitting system; (2) adapting the size and accumulation approach of nanoframework electrocatalysts to produce high-activity crystallographic features on the surfaces of different nanostructure electrocatalysts; (3) improving the surface phase to increase the active sites of nanoformat hybrids by heteroatom loading or surface adjustment; and (4) compositing the well-adjusted nanoarray morphology including nanosheets, nanorods, nanowires, with mostly revealed electrocatalytic active sites, improved stability, and enhanced electron transport. Although various groups are researching HER and OER schemes, the results are still incomplete. Thus, combining highly

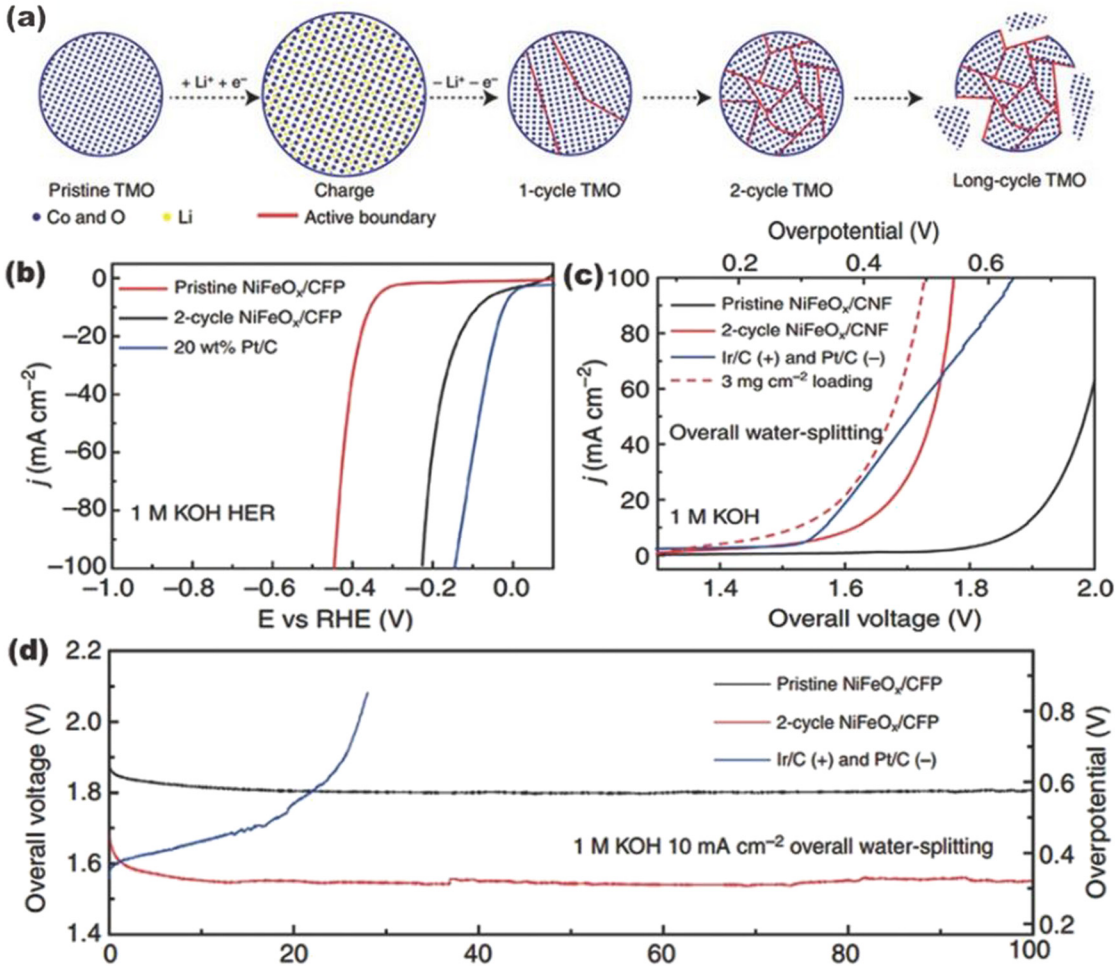

Figure 8: (a) Transition metal oxide (TMO) molecules continuously shift from single-crystalline to ultrathin correlated crystalline NPs. Stable cell loop may affect particle dispersion. (b) The HER performance of 2-loop $NiFeO_x$/CFP remarkably increased from its pristine complement. (c) Two-loop $NiFeO_x$/CFP as an HER as well as OER bifunctional electrocatalyst in basic solution (1 M KOH) for complete water splitting. (d) Long-lasting constancy of 2-loop $NiFeO_x$/CFP for HER and OER catalysts compares to Ir and Pt combination. Redrawn from [130], copyright 2015, Nature Publishing Group.

active sites, stability, and low-priced electrocatalysts with controlled overpotentials for both reactions (HER/OER) is still a challenge.

3.2.1 Transition-metal-based electrocatalysts

TMOs have been shown to be outstanding electrocatalysts for OER; they are highly soluble in acidic solutions but show static kinetics for HER in basic conditions [78,127,128]. Hence, it is still a major challenge to develop nanostructures that promote TMOs with strong activity toward both HER and OER in basic solutions. Du's group [129] reported the primitive fabrication of Co_3O_4 nanocrystals with a large surface area by pyrolysis of the $[Co(NH_3)_n]^{2+}$-oleic acid structure and consequent spray degradation. Although these nanocrystals could concurrently run both reactions (HER/OER) in basic solution due to their large electronic potentiality and defined active sites, the operating voltage for inclusive water splitting is around 1.9 V, that is sufficiently greater than the theoretical lowest value of 1.23 V. So it has high energy to develop the catalytic activities of TMOs. Cui *et al.* illustrated the fabrication of ultrasmall TMO (Ni, Fe, and Co oxides and their blends) nanoparticles with huge electrocatalytic performance for HER and OER in alkaline electrolytes [130]. This group proposed that the lithiation/delithiation method could convert pristine TMO nanoparticles (=20 nm) into shorter ones (=2–5 nm) that could notably advance the electrocatalytic efficiency (Figure 8a). Cui *et al.* also reported that the impressive activities of TMO catalysts could be because of their

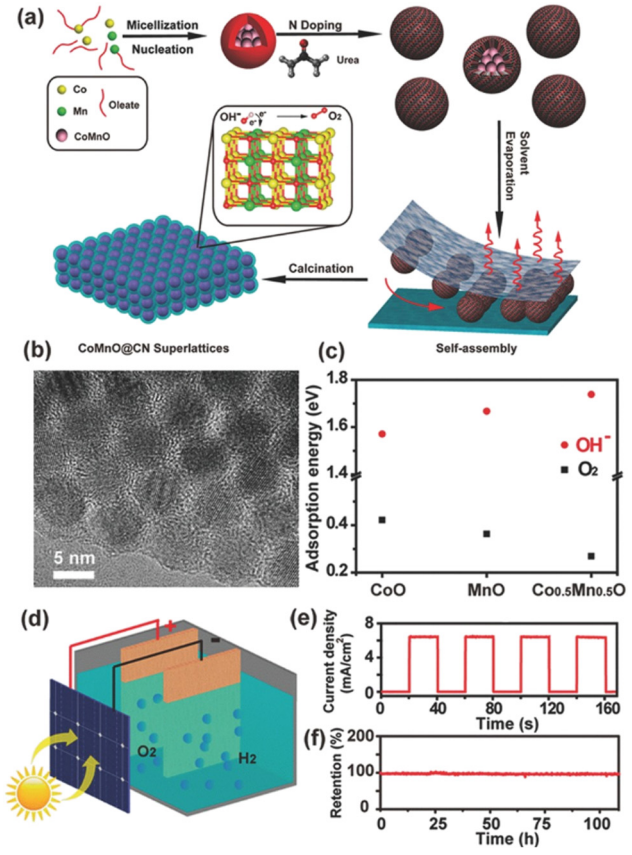

Figure 9: (a) Diagram of the CoMnO@CN super lattices formation. (b) TEM image of a CoMnO@CN super lattice. (c) Determined adsorption energies of OH^- (red dots) as well as O_2 (black dots) on CoO, MnO, and $Co_{0.5}Mn_{0.5}O$ (001) surfaces. (d) Illustration of the solar water-splitting battery without utilizing current, applying a commercial planar Si solar battery. (e) Chronoamperometry analysis of the solar water-splitting battery under AM 1.5 G artificial sunlight. (f) Long-lasting strength of that solar battery under regular sunlight for ~5 days. Reprinted from [132], copyright 2015, American Chemical Society.

catalytically active centers and abundant surface areas. Remarkably, an extensive number of lithiation/delithiation loops may cleave the pristine atoms; and if a bulky solid electrolyte connection is wrapped around the surface, it would negatively impact the catalytic performance of TMOs. The advanced $NiFeO_x$/CFP revealed high HER efficiency and also exhibited strong OER performance under basic solutions, which only needed a low overpotential (88 mV) to carry a 10-mA cm^{-2} cathodic potential (Figure 8b). Moreover, in the same electrolyte solution, the lithiation/delithiation approach generated a dramatic bifunctional $NiFeO_x$/CFP catalyst as a combined HER and OER catalysts (Figure 8a and d). Therefore, improving the particular surface phase and adjusting the surface active sites are favorable ways of improving the kinetics and decreasing the overpotential.

Another major advance is the mixture of TMOs and high-potential elements, such as metals, metal alloys, and carbon-based chemicals. Jin's group [131] prepared several multifunctional catalysts (CoO_x@NC) concurrently used for HER and OER in alkaline conditions. Although metal oxide-type catalysts have lower electrocatalytic efficiency for HER in basic conditions, Li *et al.* illustrated that a electrocatalyst of nitrogen-doped graphene covered with Co and Mn oxide (CoMnO@CN) exhibited greater HER activity than several metal sulfides (selenides and phosphates) [132]. The DFT calculation showed that the CoMnO nanoparticles could decrease the adsorption power of O_2 and also cooperatively improve the capacity for adsorbing OH^-, indicating strong OER characteristics (Figure 9c). Remarkably, the nitrogen-doped amorphous carbon structure could also provide a high electronic framework and additional active sites, consequently improving the catalytic efficiency of complete water splitting. CoMnO@CN cathodic and anodic catalysts were expanded for use in a solar energy-driven water electrolyzer and a solar to the hydrogen modification productivity of 8% was observed (Figure 9d). Interestingly a stable current density was analyzed from this electrolyzer, which was 6.43 mA cm^{-2} and correlated well with the reworked on–off loops of artificial sunlight (AM 1.5 G) (Figure 9e); a minimal decrease in current density was reported after 100 h of uninterrupted trial (Figure 9f).

3.2.2 Carbon-based catalysts

Metal-based catalysts, metal oxides, sulfides, selenides, and phosphates, are the most current evolution in the improvement of low-price and effective multi-functional electrocatalysts for both HER [133] and OER [134]. However, the major limitations of these metal-doped electrocatalysts are that they have greater resistance, they are complicated to synthesize, and their bifunctional electrochemical characteristics remain deficient [129,135–137]. From this point of view, innovative nanostructured catalysts are desired for achieving highly effective multifunctional electrocatalysts for HER and OER, which are cost-effective. Carbon nanomaterials, such as CNTs, are generally used as backing elements for HER or OER catalysts to improve the electrochemical performance [112,113,138–140]. Although these carbon nanomaterials can provide outstanding catalytic efficiency and friendly morphology beds, they were fundamentally slow-moving over the HER and OER [138,141]. Several metal-free heteroatoms, such as nitrogen, sulfur, phosphorus, boron, and

oxygen, were necessary for imbuing the low electrocatalytic pristine carbon nanomaterials with high performance [142,143]. The electrocatalytic conductivity conferred on the pristine nanomaterials with carbon can be primarily attributed to the electron-receiving performance of the added heteroatoms, which generated extra active sites and molecular species [144,145]. In 2013, Zhao's group [146] primarily studied the formation of N-rich graphite nanomaterials for OER using the pyrolysis of an N-doped carbon materials directly. These catalysts have impressive OER activity with a nominal overpotential of 0.38 V in alkaline conditions compared with various conventional electrocatalysts at a current density of 10 mA cm^{-2}. In 2014, Zheng's group [147] synthesized N and P mix-doped carbon matrix catalyst for rechargeable and effective H_2 formation under acidic and basic conditions. The DFT calculations illustrated that the addition of one couple heteroatom (N or P) could cooperatively actuate adjacent carbon atoms in the graphene framework by impacting their valence band of active carbon to induce electrocatalytic efficiency for HER. Subsequently, codopant carbon nanomaterials containing different heteroatoms have been assembled as effective and durable HER and OER electrocatalysts. Notably, Xu *et al*. prepared a multidoped (N, P, and O) porous graphite carbon@oxidized carbon cloth (ONPPGC/OCC) as bifunctional electrocatalyst for complete water splitting [148]. This ONPPGC/OCC requires a nominal overpotential of 410 mV for OER electrocatalysis to reach 10 mA cm^{-2} current density and long-lasting electrochemical efficiency. The OER kinetics were also measured by the Tafel slope which was 83 mV dec^{-1} for ONPPGC/OCC. The Tafel slope of ONPPGC/OCC is lower than that of bare GC (423 mA dec^{-1}) and Pt/C (86 mA dec^{-1}). Interestingly, this 3D porous material not only displays sufficient electrocatalytic activity in a basic water electrolyzer which is achieved at 10 mA cm^{-2} for a 1.66 V cell voltage but also high electrocatalytic performance under both acidic and neutral solutions. The outstanding hydrogen and OER electrocatalytic efficiency would be fundamentally attributable to the following critical aspects: the huge potentiality of graphitized carbon; the particular 3D porous structure between PGC and OCC; and the addition of lone pair electron-based P and N. This research has revealed the possibility of enhancing greatly effective and low-price bifunctional electrochemicals, which depend on metal-free nanomaterials for both HER and OER.

3.2.3 Transition-metal-based dichalcogenides and phosphides

Transition metal dichalcogenides (TMDs), such as metal sulfides and metal selenides, have layer structures similar to that of graphite, and a large effort has been put forth to improve TMDs for electrocatalysis of both HER and OER in basic conditions [149–155]. The phosphorus in the framework and the reaction intermediates made TMDs suitable for HER and OER [156–159]. However, the electrochemical activities of these catalysts are mostly depend on how they are fabricated. Simultaneously, synthesizing 3D nanostructures with more crystallographic features and large active sites are crucial for improving the multifunctional electrocatalysts for HER and OER. For example, Shalom *et al*. revealed a nano-framework-type nickel phosphide (Ni_5P_4) foil that was directly assembled on a nickel substrate as a bifunctional electrocatalyst [158]. The high performance of this Ni_5P_4 foil in alkaline solution may be attributable to the 3D structure that can assist the fabrication of NiOOH on Ni_5P_4 heterojunction and the subsequent development of electrochemical activities. Feng *et al*. [160] primarily synthesized {210} high-record phase nickel sulfide (Ni_3S_2) nanosheets and nickel foam (NF) named Ni_3S_2/NF. This type of electrocatalyst was fabricated by the direct vulcanization of NF and prepared as a developed, coverless, and multifunctional electrocatalyst for HER and OER. They reported that cooperation between Ni_3S_2 nano-framework and its favorable high-record surface could expose large numbers of active centers, greatly improving the desorption of water molecules.

Moreover, Feng *et al*. [161] reported another promising development a 3D hybrid catalyst containing three different components including nonstoichiometric $Co_{0.85}Se$, covered carbon film, and NiFe-coated double-hydroxide (NiFe-LDH), which had high HER and OER activity in alkaline media. They suggested that the nonstoichiometric $Co_{0.85}Se$ carries enough active sites, and the NiFe-LDH is characterized by special coated framework, whereas the electrochemical performance and durability can be improved for complete water splitting in alkaline conditions. Furthermore, the covered graphene foil not only offered conductive elements to improve the charge exchange between the electrode and the catalyst ($Co_{0.85}Se$/NiFe-LDH) but also involved extensive outlying surfaces for selenide production. The calculated composition allows additional active sites, a high surface area,

and more activity, promising outstanding HER and OER activities in the carbon film/$Co_{0.85}Se$/NiFe-LDH catalyst. Recently, Zhang *et al.* [162] developed a core-case hybrid process, which comprises cobalt sulfide, molybdenum disulfide, and graphene nanofibers (named Co_9S_8@MoS_2/CNFs) as a mostly stable and long-lasting 3D electrode for both HER and OER. The particular Co_9S_8@MoS_2 core-case nanostructure consists of a nucleus of cobalt sulfide nanoparticles fully encased in molybdenum disulfide (Figure 10a and b). Connecting the favorable characteristics of a particular step, the Co_9S_8@MoS_2/CNF displays notably developed HER and OER characteristics (Figure 10c and d), corresponding to the most notable nonnoble nanomaterial-type HER and OER electrocatalysts.

4 Trifunctional metal-free electrocatalysts for the ORR, OER, and HER

The ORR, OER, and HER are the predominant half-cell energy conversion technologies. In 2013, Jahan's group [163] fabricated a compound consisting of graphene oxide and a copper-based organometallic structure (GO/Cu-MOF) with favorable ORR/OER/HER efficiency in acidic solution (0.5 M H_2SO_4). Although the GO/Cu-MOF can perform ORR/OER/HER in a similar electrode, the electrochemical performance is still inadequate. Later, Hou's group [164] synthesized a composite catalyst made of a nitrogen-based carbon/cobalt-enclosed porous graphene polyhedron, which demonstrated outstanding catalytic behavior for the ORR (high activity and the four-electron route) and OER which showed 1.66 V overpotential for 10 mA cm^{-2} in alkaline conditions and high efficiency for HER (58 mV initial overpotential) in acidic conditions. Moreover, Liu *et al.* [165] reported a multielement trifunctional Co-CoO/N-rGO catalysts for ORR/OER/HER in basic conditions. In 2019, Li's group [166] reported an impulsive gas-foaming process to synthesize nitrogen-based ultrathin carbon nanosheets (NCNs) by easy pyrolysis of a combination of citric acid and NH_4Cl that demonstrates inferior overpotential and potent activity for the ORR, OER, and HER. They also demonstrated that the innate active sites for the electrochemical reactions (ORR, OER, and HER) are the carbon atoms established at the rich-edge defects and alongside the carbon N dopants. DFT calculations

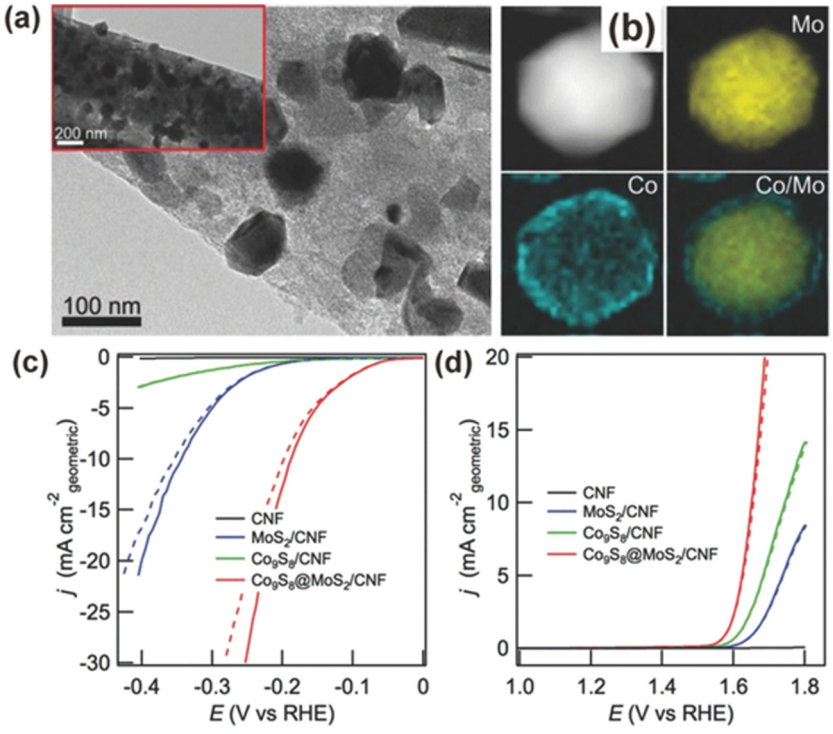

Figure 10: (a) TEM figures of Co_9S_8@MoS_2/CNF. (b) STEM-EDS mapping of the same catalyst. (c) HER performance of CNF, MoS_2/CNF, Co_9S_8/CNF, and Co_9S_8@MoS_2/CNF at 2 mV s^{-1} in acid solution (0.5 M H_2SO_4) (d) OER efficiency of CNF, MoS_2/CNF, Co_9S_8/CNF, and Co_9S_8@MoS_2/CNF at 2 mV s^{-1} in basic solution (1 M KOH). All the outcomes illustrated by solid lines were associated with iR losses. The dotted lines display the initial events. Reprinted from [160], copyright 2015, Wiley-VCH.

illustrated that carbon N dopants and the large graphene-edge defects in the porous framework are accountable for the multifunctional electrochemical efficiency of NCN-1000-5. This research not only presents a functional approach for the continual improvement of progressive carbon nanomaterials with ultrahigh particular surface areas and plentiful edge defects but also supports important guidance for fabricating and improving trifunctional metal-free electrocatalysts for different power-associated electrochemical reactions. They demonstrated the electrocatalytic behavior of different active sites for the ORR and OER in acidic solutions (pH = 0) by analyzing their overpotential (η) corresponding to the $4e^-$ route. Results are shown in Figure 11a, which represent the volcano curves of ORR and OER overpotentials *vs* ΔG(*O) for different active sites on the N-doped carbon single layer, reclining and zigzag carbon nanoribbons. The most effective active site examined was the carbon molecule for the ORR, which was located at the reclining nanoribbon outline and next to the carbon N-dopant (A-1, Figure 11b). The most effective active phase for the OER was near the graphitic N dopant and the carbon atom, which is 3.34 Å away from the reclining ribbon edge (Figure 11c). Li *et al.* demonstrated three types of N dopants, including graphitic N (1gN-1), pyridinic N (1pdN-1), and pyrrolic N (1prN-1) in Figure 11a. The key factor in improving the ORR/OER performance for carbon nanosheets was performed by 1gN-1 [167,168]. Interestingly, the most active site for the ORR (A-1) was also the best for HER performance, where the ΔG(*H) value was 0.07 eV at a hydrogen analysis of 2.27% (Figure 11d). The outstanding facilities of nitrogen-doped carbon nanosheets (NCN-1000-5) enhanced the multifunctional electrochemical performance of concurrent ORR, OER, and HER because of their plentiful micropores edge defects, exclusive ultrathin nanosheet structures, and their large surface areas.

5 Conclusions and outlook

The composition of dynamic, impressive, durable, and earth-abundant catalysts for electrochemical reactions (*e.g.*, ORR, OER, and HER) is a significant challenge. However, the implementation of bifunctional catalysts for ORR/OER and HER/OER has the great advantage of decreasing the price and shortening the process. Additionally, DFT calculations can support more instinctive and proper insights into the full electrochemical reaction method and allow some applicable predictions to be made, allowing for the logical structure and composition of different nanostructured electrocatalysts with high efficiency. Therefore, it is interesting to develop encouraging low-cost and highly effective catalysts that can concurrently assemble the ORR/OER or HER/OER for sustainable technologies. The aim of this review was to provide an outlook on the current evolution of developed nanomaterial electrocatalysts for the ORR/OER and HER/OER. Multifunctional electrochemical performance was examined as a significant area in nanomaterial research. Unfortunately, the high price and defined activity of metal-doped electrocatalysts have hindered the extensive utilization of multifunctional catalysts in the rechargeable energy sectors. The review supports the substitution of expensive metal-doped catalysts with the stable inexpensive electrocatalysts for fuel cell and metal–air batteries to achieve energy in a low price and expandable way. Due to their high-potential activities, carbon-doped

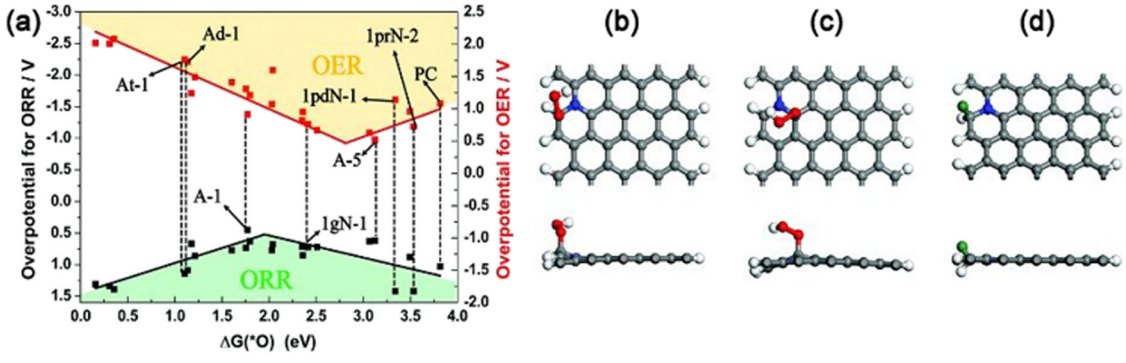

Figure 11: (a) Volcano plots for the ORR and OER are prepared by sketching the overpotential as the action of ΔG(*O) at different available active sites. Top and side perspectives of active site (b) A-1 is shown for the ORR, (c) A-3 is shown for the OER, and (d) A-1 is shown for the HER, the green ball performing the adsorbed H (θ = 2.27%). Reprinted from [166], copyright 2019, Royal Society of Chemistry.

composite catalysts usually provide high electrochemical conductivity. The main target has been inspired by the improvement in low price and high-performance catalysts, including perovskites, metal phosphides, sulfides, carbides, or nitrides, and graphene-doped electrocatalysts, to bypass the applying of the traditional, high-price noble metals of low activity, including Pt, RuO_2, and IrO_2. Multifunctional nanostructures promoted outstanding portability, solubility, structural tunability, and the utility of tailoring the surface characteristics in remarkable ways to achieve high electrocatalytic performance. Our groups are studying nanomaterial carbon composites to be used to electrochemical reactions. Composite frameworks have revealed the real activity achieved in terms of energy consistency and durability; further developed formation processes are needed for use in the operation of the future generations of fuel cells and devices.

Funding information: The Technological Innovation R&D Program (S2848103) funded by the Small and Medium Business Administration (SMBA, Korea) and supported by the Korea Sanhak Foundation (KSF) in 2020, entitled "Development of high-performance carbon-based adsorption material technology to remove indoor harmful factors" are greatly appreciated.

Author contributions: All authors have accepted responsibility for the entire content of this manuscript and approved its submission.

Conflict of interest: The authors state no conflict of interest.

References

[1] Chu S, Majumdar A. Opportunities and challenges for a sustainable energy future. Nature. 2012;488(7411):294–303.
[2] Ali R, Shan A, Saranya G, Jian X, Mahmood A, Mahmood N, et al. Bifunctional water-electrolysis-catalysts meeting band-diagram analysis: case study of "FeP" electrodes. J Mater Chem A. 2020;8(38):20021–9.
[3] Yang G, Park S-J. Single-step solid-state synthesis and characterization of $Li_4Ti_{5-x}Fe_xO_{12-y}$ ($0 \le x \le 0.1$) as an anode for lithium-ion batteries. J Mater Chem A. 2020;8(5):2627–36.
[4] Tahir M, Pan L, Idrees F, Zhang X, Wang L, Zou J-J, et al. Electrocatalytic oxygen evolution reaction for energy conversion and storage: a comprehensive review. Nano Energy. 2017;37:136–57.
[5] Sun H, Heo Y-J, Park J-H, Rhee KY, Park S-J. Advanced in layered double hydroxide-based ternary nanocomposites for photocatalysis of contaminants in water. Nanotechnol Rev. 2020;9(1):1381–96.
[6] Pan Y, Xu K, Wu C. Recent progress in supercapacitors based on the advanced carbon electrodes. Nanotechnol Rev. 2019;8(1):299–314.
[7] Jiang H, Li J, Liang M, Deng H, Zhou Z. Superior Fe_xN electrocatalyst derived from 1,1′-diacetylferrocene for oxygen reduction reaction in alkaline and acidic media. Nanotechnol Rev. 2020;9(1):843–52.
[8] Bu L, Zhang N, Guo S, Zhang X, Li J, Yao J, et al. Biaxially strained PtPb/Pt core/shell nanoplate boosts oxygen reduction catalysis. Science. 2016;354(6318):1410–4.
[9] Seitz LC, Dickens CF, Nishio K, Hikita Y, Montoya J, Doyle A, et al. A highly active and stable $IrO_x/SrIrO_3$ catalyst for the oxygen evolution reaction. Science. 2016;353(6303):1011–4.
[10] Wang H, Abruña HD. IrPdRu/C as H_2 oxidation catalysts for alkaline fuel cells. J Am Chem Soc. 2017;139(20):6807–10.
[11] Stoerzinger KA, Diaz-Morales O, Kolb M, Rao RR, Frydendal R, Qiao L, et al. Orientation-dependent oxygen evolution on RuO_2 without lattice exchange. ACS Energy Lett. 2017;2(4):876–81.
[12] Li Y, Xiong D, Liu Y, Liu M, Liu J, Liang C, et al. Correlation between electrochemical performance degradation and catalyst structural parameters on polymer electrolyte membrane fuel cell. Nanotechnol Rev. 2019;8(1):493–502.
[13] Zhu W, Zhang R, Qu F, Asiri AM, Sun X. Design and Application of Foams for Electrocatalysis. ChemCatChem. 2017;9(10):1721–43.
[14] Sun T, Liu P, Zhang Y, Chen Z, Zhang C, Guo X, et al. Boosting the electrochemical water splitting on Co_3O_4 through surface decoration of epitaxial S-doped CoO layers. Chem Eng J. 2020;390:124591.
[15] Galani SM, Mondal A, Srivastava DN, Panda AB. Development of RuO_2/CeO_2 heterostructure as an efficient OER electrocatalyst for alkaline water splitting. Int J Hydrog Energy. 2020;45(37):18635–44.
[16] Yin J, Li Y, Lv F, Fan Q, Zhao Y-Q, Zhang Q, et al. NiO/CoN porous nanowires as efficient bifunctional catalysts for Zn-air batteries. ACS Nano. 2017;11(2):2275–83.
[17] Pei Z, Gu J, Wang Y, Tang Z, Liu Z, Huang Y, et al. Component matters: paving the roadmap toward enhanced electrocatalytic performance of graphitic C_3N_4-based catalysts via atomic tuning. ACS Nano. 2017;11(6):6004–14.
[18] Wang C, Wang F, Zhang L-S, Qiu S-Y, Gu L-L, Wang K-X, et al. Multi-dimensionally hierarchical self-supported $Cu@Cu_{2+1}O@Co_3O_4$ heterostructure enabling superior lithium-ion storage and electrocatalytic oxygen evolution. Chem Eng J. 2021;405:126699.
[19] Cano ZP, Banham D, Ye S, Hintennach A, Lu J, Fowler M, et al. Batteries and fuel cells for emerging electric vehicle markets. Nat Energy. 2018;3(4):279–89.
[20] Tian N, Lu BA, Yang XD, Huang R, Jiang YX, Zhou ZY, et al. Rational design and synthesis of low-temperature fuel cell electrocatalysts. Electrochem Energy Rev. 2018;1(1):54–83.
[21] Huang Z-F, Wang J, Peng Y, Jung C-Y, Fisher A, Wang X. Design of efficient bifunctional oxygen reduction/evolution electrocatalyst: recent advances and perspectives. Adv Energy Mater. 2017;7(23):1700544(1–21).
[22] Ghosh S, Basu RN. Multifunctional nanostructured electrocatalysts for energy conversion and storage: current status and perspectives. Nanoscale. 2018;10(24):11241–80.

[23] Kuang M, Zheng G. Nanostructured bifunctional redox electrocatalysts. Small. 2016;12(41):5656–75.
[24] Xu H, Ci S, Ding Y, Wang G, Wen Z. Recent advances in precious metal-free bifunctional catalysts for electrochemical conversion systems. J Mater Chem A. 2019;7(14):8006–29.
[25] Li C, Liu H, Yu Z. Novel and multifunctional inorganic mixing salt-templated 2D ultrathin Fe/Co-N/S-carbon nanosheets as effectively bifunctional electrocatalysts for Zn-air batteries. Appl Catal B Env. 2019;241:95–103.
[26] Chen C, Kang Y, Huo Z, Zhu Z, Huang W, Xin HL, et al. Highly crystalline multimetallic nanoframes with three-dimensional electrocatalytic surfaces. Science. 2014;343:1339–43.
[27] Li S, Hao X, Abudula A, Guan G. Nanostructured co-based bifunctional electrocatalysts for energy conversion and storage: current status and perspectives. J Mater Chem A. 2019;7(32):18974–707.
[28] Laalioui S, Alaoui KB, Dads HA, Assali KE, Ikken B, Outzourhit A. Progress in perovskite based solar cells: scientific and engineering state of the art. Rev Adv Mater Sci. 2020;59(1):10–25.
[29] Oku T. Crystal structures of perovskite halide compounds used for solar cells. Rev Adv Mater Sci. 2020;59(1):264–305.
[30] Ding J, Wang P, Ji S, Wang H, Linkov V, Wang R. N-doped mesoporous FeN_x/carbon as ORR and OER bifunctional electrocatalyst for rechargeable zinc-air batteries. Electrochim Acta. 2019;296:653–61.
[31] Guo Y, Dai Z, Lu J, Zeng X, Yuan Y, Bi X, et al. Lithiation-induced non-noble metal nanoparticles for Li-O_2 batteries. ACS Appl Mater Interfaces. 2019;11(1):811–8.
[32] Gozalzadeh S, Nasirpouri F, Seok SI. Dimethyformamide-free synthesis and fabrication of lead halide perovskite solar cells from electrodeposited PbS precursor films. Chem Eng J. 2021;411:128460.
[33] Lu Y, Li Z, Xu Y, Tang L, Xu S, Li D, et al. Bimetallic Co–Mo nitride nanosheet arrays as high-performance bifunctional electrocatalysts for overall water splitting. Chem Eng J. 2021;411:128433.
[34] Sun H, Tian C, Fan G, Qi J, Liu Z, Yan Z, et al. Boosting activity on Co_4N porous nanosheet by coupling CeO_2 for efficient electrochemical overall water splitting at high current densities. Adv Funct Mater. 2020;30(32):1–14.
[35] Naghib SM, Zare Y, Rhee KY. A facile and simple approach to synthesis and characterization of methacrylated graphene oxide nanostructured polyaniline nanocomposites. Nanotechnol Rev. 2020;9(1):53–60.
[36] Liang H, Gandi AN, Xia C, Hedhili MN, Anjum DH, Schwingenschlögl U, et al. Amorphous NiFe-OH/NiFeP electrocatalyst fabricated at low temperature for water oxidation applications. ACS Energy Lett. 2017;2(5):1035–42.
[37] Wang C, Wang F, Qiu S-Y, Gao J, Gu L-L, Wang K-X, et al. Integrating Co_3O_4 nanoparticles with MnO_2 nanosheets as bifunctional electrocatalysts for water splitting. Int J Hydrog Energy. 2021;46:10356–65.
[38] Hu C, Dai L. multifunctional carbon-based metal-free electrocatalysts for simultaneous oxygen reduction, oxygen evolution, and hydrogen evolution. Adv Mater. 2017;29(9):1–9.
[39] Sun J, Lowe SE, Zhang L, Wang Y, Pang K, Wang Y, et al. Ultrathin nitrogen-doped holey carbon@graphene bifunctional electrocatalyst for oxygen reduction and evolution reactions in alkaline and acidic media. Angew Chem, Int Ed. 2018;57(50):16511–5.
[40] Zhou M, Wang HL, Guo S. Towards high-efficiency nanoelectrocatalysts for oxygen reduction through engineering advanced carbon nanomaterials. Chem Soc Rev. 2016;45(5):1273–307.
[41] Lyu YQ, Ciucci F. Activating the bifunctionality of a perovskite oxide toward oxygen reduction and oxygen evolution reactions. ACS Appl Mater Interfaces. 2017;9(41):35829–36.
[42] Wu G, More KL, Johnston CM, Zelenay P. High-performance electrocatalysts for oxygen reduction derived from polyaniline, iron, and cobalt. Science. 2011;332(6028):443–7.
[43] Gu X, Liu Z, Liu H, Pei C, Feng L. Fluorination of ZIF-67 framework template Prussian blue analogue nano-box for efficient electrochemical oxygen evolution reaction. Chem Eng J. 2021;403:126371.
[44] Seh ZW, Kibsgaard J, Dickens CF, Chorkendorff I, Norskov JK, Jaramillo TF. Combining theory and experiment in electrocatalysis: insights into materials design. Science. 2017;355(6321):eaad4998.
[45] Xia W, Mahmood A, Liang Z, Zou R, Guo S. Earth-abundant nanomaterials for oxygen reduction. Angew Chem, Int Ed. 2016;55(8):2650–76.
[46] Koper MT. Theory of the transition from sequential to concerted electrochemical proton–electron transfer. Phys Chem Chem Phys. 2013;15(5):1399–407.
[47] Gu P, Zheng M, Zhao Q, Xiao X, Xue H, Pang H. Rechargeable zinc-air batteries: a promising way to green energy. J Mater Chem A. 2017;5(17):7651–66.
[48] Nie Y, Li L, Wei Z. Recent advancements in Pt and Pt-free catalysts for oxygen reduction reaction. Chem Soc Rev. 2015;44(8):2168–201.
[49] Chandel VS, Wang G, Talha M. Advances in modelling and analysis of nano structures: a review. Nanotechnol Rev. 2020;9(1):230–58.
[50] Anderson AB, Roques J, Stamenkovic V. Activation energies for oxygen reduction on platinum alloys: theory and experiment. J Phys Chem B. 2005;109(3):1198–203.
[51] Zhang J, Huang Z, He C, Zhang J, Mei P, Han X, et al. Binary carbon-based additives in $LiFePO_4$ cathode with favorable lithium storage. Nanotechnol Rev. 2020;9(1):934–44.
[52] Ren S, Duan X, Liang S, Zhang M, Zheng H. Bifunctional electrocatalysts for Zn-air batteries: recent developments and future perspectives. J Mater Chem A. 2020;8(13):6144–82.
[53] Wang G, Chen Q, Gao M, Yang B, Hui D. Generalized locally-exact homogenization theory for evaluation of electric conductivity and resistance of multiphase materials. Nanotechnol Rev. 2020;9(1):1–16.
[54] Anderson AB, Albu TV. *Ab initio* approach to calculating activation energies as functions of electrode potential: trial application to four-electron reduction of oxygen. Electrochem Commun. 1999;1(6):203–6.
[55] Toda T, Igarashi H, Uchida H, Watanabe M. Enhancement of the electroreduction of oxygen on Pt Alloys with Fe, Ni, and Co. J Electrochem Soc. 1999;146(10):3750–6.
[56] Yeh KY, Janik MJ. Density functional theory-based electrochemical models for the oxygen reduction reaction: comparison of modeling approaches for electric field and solvent effects. J Comput Chem. 2011;32(16):3399–408.

[57] He W, Wang Y, Jiang C, Lu L. Structural effects of a carbon matrix in nonprecious metal O_2-reduction electrocatalysts. Chem Soc Rev. 2016;45(9):2396–409.
[58] Wang D, Xin HL, Hovden R, Wang H, Yu Y, Muller DA, et al. Structurally ordered intermetallic platinum–cobalt core-shell nanoparticles with enhanced activity and stability as oxygen reduction electrocatalysts. Nat Mater. 2013;12(1):81–7.
[59] Liu J, Jiao M, Mei B, Tong Y, Li Y, Ruan M, et al. Carbon-supported divacancy-anchored platinum single-atom electrocatalysts with superhigh Pt utilization for the oxygen reduction reaction. Angew Chem. 2019;131(4):1175–9.
[60] Wang ZL, Xu D, Xu JJ, Zhang XB. Oxygen electrocatalysts in metal-air batteries: from aqueous to nonaqueous electrolytes. Chem Soc Rev. 2014;43(22):7746–86.
[61] Mahmood N, Tahir M, Mahmood A, Zhu J, Cao C, Hou Y. Chlorine-doped carbonated cobalt hydroxide for supercapacitors with enormously high pseudocapacitive performance and energy density. Nano Energy. 2015;11:267–76.
[62] Tahir M, Mahmood N, Zhang X, Mahmood T, Butt FK, Aslam I, et al. Bifunctional catalysts of Co_3O_4@GCN tubular nanostructured (TNS) hybrids for oxygen and hydrogen evolution reactions. Nano Res. 2015;8(11):3725–36.
[63] Meng C, Ling T, Ma TY, Wang H, Hu Z, Zhou Y, et al. Atomically and electronically coupled pt and coo hybrid nanocatalysts for enhanced electrocatalytic performance. Adv Mater. 2017;29:1604607.
[64] Lv Z, Mahmood N, Tahir M, Pan L, Zhang X, Zou JJ. Fabrication of zero to three dimensional nanostructured molybdenum sulfides and their electrochemical and photocatalytic applications. Nanoscale. 2016;8(43):18250–69.
[65] Huang ZF, Song J, Li K, Tahir M, Wang YT, Pan L, et al. Hollow cobalt-based bimetallic sulfide polyhedra for efficient All-pH-Value electrochemical and photocatalytic hydrogen evolution. J Am Chem Soc. 2016;138(4):1359–65.
[66] Fabbri E, Habereder A, Waltar K, Kötz R, Schmidt TJ. Developments and perspectives of oxide-based catalysts for the oxygen evolution reaction. Catal Sci Technol. 2014;4:3800–21.
[67] Suen NT, Hung SF, Quan Q, Zhang N, Xu YJ, Chen HM. Electrocatalysis for the oxygen evolution reaction: recent development and future perspectives. Chem Soc Rev. 2017;46(2):337–65.
[68] Yan P, Huang M, Wang B, Wan Z, Qian M, Yan H, et al. Oxygen defect-rich double-layer hierarchical porous Co_3O_4 arrays as high-efficient oxygen evolution catalyst for overall water splitting. J Energy Chem. 2020;47:299–306.
[69] Wang J, Xu F, Jin H, Chen Y, Wang Y. Non-noble metal-based carbon composites in hydrogen evolution reaction: fundamentals to applications. Adv Mater. 2017;29(14):1605838.
[70] Zhao G, Rui K, Dou SX, Sun W. Heterostructures for electrochemical hydrogen evolution reaction: a review. Adv Funct Mater. 2018;28(43):1–26.
[71] Mahmood N, Yao Y, Zhang JW, Pan L, Zhang X, Zou JJ. Electrocatalysts for hydrogen evolution in alkaline electrolytes: mechanisms, challenges, and prospective solutions. Adv Sci. 2018;5(2):1700464.
[72] Fang M, Dong G, Wei R, Ho JC. Hierarchical nanostructures: design for sustainable water splitting. Adv Energy Mater. 2017;7(23):1700559.
[73] Wu ZS, Yang S, Sun Y, Parvez K, Feng X, Müllen K. 3D nitrogen-doped graphene aerogel-supported Fe_3O_4 nanoparticles as efficient electrocatalysts for the oxygen reduction reaction. J Am Chem Soc. 2012;134(22):9082–5.
[74] Wang HY, Hsu YY, Chen R, Chan TS, Chen HM, Liu B. Ni^{3+}-induced formation of active NiOOH on the spinel Ni-Co oxide surface for efficient oxygen evolution reaction. Adv Energy Mater. 2015;5(10):15000091.
[75] Wang C, Liu Y, Li Z, Wang L, Niu X, Sun P. Novel space-confinement synthesis of two-dimensional Fe, N-codoped graphene bifunctional oxygen electrocatalyst for rechargeable air-cathode. Chem Eng J. 2021;411:128492.
[76] Huang K, Wang R, Zhao S, Du P, Wang H, Wei H, et al. Atomic species derived CoO_x clusters on nitrogen doped mesoporous carbon as advanced bifunctional electro-catalysts for Zn-air battery. Energy Storage Mater. 2020;29:156–62.
[77] Song S, Li W, Deng Y-P, Ruan Y, Zhang Y, Qin X, et al. TiC supported amorphous MnO_x as highly efficient bvifunctional electrocatalyst for corrosion resistant oxygen electrode of Zn-air batteries. Nano Energy. 2020;67:104208.
[78] Hu X, Cheng F, Zhang N, Han X, Chen J. Nanocomposite of Fe_2O_3@C@MnO_2 as an efficient cathode catalyst for rechargeable lithium–oxygen batteries. Small. 2015;11(41):5545–50.
[79] Aijaz A, Masa J, Rösler C, Antoni H, Fischer RA, Schuhmann W, et al. MOF-templated assembly approach for Fe_3C nanoparticles encapsulated in bamboo-like N-doped CNTs: highly efficient oxygen reduction under acidic and basic conditions. Chem- A Eur J. 2017;23(50):12125–30.
[80] Liu L, Wang J, Hou Y, Chen J, Liu HK, Wang J, et al. Self-assembled 3D foam-like $NiCo_2O_4$ as efficient catalyst for lithium oxygen batteries. Small. 2016;12(5):602–11.
[81] Yan W, Yang Z, Bian W, Yang R. $FeCo_2O_4$/hollow graphene spheres hybrid with enhanced electrocatalytic activities for oxygen reduction and oxygen evolution reaction. Carbon N Y. 2015;92:74–83.
[82] Yang Y, Yin W, Wu S, Yang X, Xia W, Shen Y, et al. Perovskite-type LaSrMnO electrocatalyst with uniform porous structure for an efficient Li–O_2 battery cathode. ACS Nano. 2016;10(1):1240–8.
[83] Liu S, Li L, Ahn HS, Manthiram A. Delineating the roles of Co_3O_4 and N-doped carbon nanoweb (CNW) in bifunctional Co_3O_4/CNW catalysts for oxygen reduction and oxygen evolution reactions. J Mater Chem A. 2015;3(21):11615–23.
[84] Jung JI, Jeong HY, Kim MG, Nam G, Park J, Cho J. Fabrication of $Ba_{0.5}Sr_{0.5}Co_{0.8}Fe_{0.2}O_{3-\delta}$ catalysts with enhanced electrochemical performance by removing an inherent heterogeneous surface film layer. Adv Mater. 2015;27(2):266–71.
[85] Maiyalagan T, Jarvis KA, Therese S, Ferreira PJ, Manthiram A. Spinel-type lithium cobalt oxide as a bifunctional electrocatalyst for the oxygen evolution and oxygen reduction reactions. Nat Commun. 2014;5:3949.
[86] Lu Z, Wang H, Kong D, Yan K, Hsu PC, Zheng G, et al. Electrochemical tuning of layered lithium transition metal oxides for improvement of oxygen evolution reaction. Nat Commun. 2014;5:4345.
[87] Chen X, Yan Z, Yu M, Sun H, Liu F, Zhang Q, et al. Spinel oxide nanoparticles embedded in nitrogen-doped carbon nanofibers as a robust and self-standing bifunctional oxygen

cathode for Zn-air batteries. J Mater Chem A. 2019;7(43):24868–76.
[88] Xu N, Zhang Y, Zhang T, Liu Y, Qiao J. Efficient quantum dots anchored nanocomposite for highly active ORR/OER electrocatalyst of advanced metal-air batteries. Nano Energy. 2019;57:176–85.
[89] Menezes PW, Indra A, González-Flores D, Sahraie NR, Zaharieva I, Schwarze M, et al. High-performance oxygen redox catalysis with multifunctional cobalt oxide nanochains: morphology-dependent activity. ACS Catal. 2015;5(4):2017–27.
[90] Wang H, Yang Y, Liang Y, Zheng G, Li Y, Cui Y, et al. Rechargeable Li–O_2 batteries with a covalently coupled $MnCo_2O_4$-graphene hybrid as an oxygen cathode catalyst. Energy Env Sci. 2012;5(7):7931–5.
[91] Bian W, Yang Z, Strasser P, Yang R. A $CoFe_2O_4$/graphene nanohybrid as an efficient bi-functional electrocatalyst for oxygen reduction and oxygen evolution. J Power Sources. 2014;250:196–203.
[92] Du J, Chen C, Cheng F, Chen J. Rapid synthesis and efficient electrocatalytic oxygen reduction/evolution reaction of $CoMn_2O_4$ nanodots supported on graphene. Inorg Chem. 2015;54(11):5467–74.
[93] Lin Y, Yang L, Zhang Y, Jiang H, Xiao Z, Wu C, et al. Defective carbon–CoP nanoparticles hybrids with interfacial charges polarization for efficient bifunctional oxygen electrocatalysis. Adv Energy Mater. 2018;8(18):1–7.
[94] Ahn SH, Manthiram A. Cobalt phosphide coupled with heteroatom-doped nanocarbon hybrid electroctalysts for efficient, long-life rechargeable zinc–air batteries. Small. 2017;13(40):1–11.
[95] Yang S, He Q, Wang C, Jiang H, Wu C, Zhang Y, et al. Confined bimetallic phosphide within P, N co-doped carbon layers towards boosted bifunctional oxygen catalysis. J Mater Chem A. 2018;6(24):11281–7.
[96] Liang Y, Li Y, Wang H, Zhou J, Wang J, Regier T, et al. Co_3O_4 nanocrystals on graphene as a synergistic catalyst for oxygen reduction reaction. Nat Mater. 2011;10(10):780–6.
[97] Li C, Han X, Cheng F, Hu Y, Chen C, Chen J. Phase and composition controllable synthesis of cobalt manganese spinel nanoparticles towards efficient oxygen electrocatalysis. Nat Commun. 2015;6:4–11.
[98] Wang H, Xu W, Richins S, Liaw K, Yan L, Zhou M, et al. Polymer-assisted approach to LaCo1-xNixO_3 network nanostructures as bifunctional oxygen electrocatalysts. Electrochim Acta. 2019;296:945–53.
[99] Bie S, Zhu Y, Su J, Jin C, Liu S, Yang R, et al. One-pot fabrication of yolk-shell structured $La_{0.9}Sr_{0.1}CoO_3$ perovskite microspheres with enhanced catalytic activities for oxygen reduction and evolution reactions. J Mater Chem A. 2015;3(4):22448–53.
[100] Lee DU, Xu P, Cano ZP, Kashkooli AG, Park MG, Chen Z. Recent progress and perspectives on bi-functional oxygen electrocatalysts for advanced rechargeable metal-air batteries. J Mater Chem A. 2016;4(19):7107–34.
[101] Elumeeva K, Masa J, Sierau J, Tietz F, Muhler M, Schuhmann W. Perovskite-based bifunctional electrocatalysts for oxygen evolution and oxygen reduction in alkaline electrolytes. Electrochim Acta. 2016;208:25–32.
[102] Risch M, Stoerzinger KA, Maruyama S, Hong WT, Takeuchi I, Shao-Horn Y. $La_{0.8}Sr_{0.2}MnO_{3-\delta}$ decorated with $Ba_{0.5}Sr_{0.5}Co_{0.8}Fe_{0.2}O_{3-\delta}$: a bifunctional surface for oxygen electrocatalysis with enhanced stability and activity. J Am Chem Soc. 2014;136(14):5229–32.
[103] Fabbri E, Nachtegaal M, Cheng X, Schmidt TJ. Superior bifunctional electrocatalytic activity of $Ba_{0.5}Sr_{0.5}Co_{0.8}Fe_{0.2}O_{3-\delta}$/carbon composite electrodes: insight into the local electronic structure. Adv Energy Mater. 2015;5(17):1–5.
[104] Zhao Y, Xu L, Mai L, Han C, An Q, Xu X, et al. Hierarchical mesoporous perovskite $La_{0.5}Sr_{0.5}CoO_{2.91}$ nanowires with ultrahigh capacity for Li-air batteries. Proc Natl Acad Sci U S A. 2012;109(48):19569–74.
[105] Jung JI, Park S, Kim MG, Cho J. Tunable internal and surface structures of the bifunctional oxygen perovskite catalysts. Adv Energy Mater. 2015;5(24):1–7.
[106] Chen CF, King G, Dickerson RM, Papin PA, Gupta S, Kellogg WR, et al. Oxygen-deficient $BaTiO_{3-x}$ perovskite as an efficient bifunctional oxygen electrocatalyst. Nano Energy. 2015;13:423–32.
[107] Cheng X, Fabbri E, Nachtegaal M, Castelli IE, Kazzi ElM, Haumont R, et al. Oxygen evolution reaction on $La_{1-x}Sr_xCoO_3$ perovskites: a combined experimental and theoretical study of their structural, electronic, and electrochemical properties. Chem Mater. 2015;27(22):7662–72.
[108] Jung J-I, Jeong HY, Lee J-S, Kim MG, Cho J. A bifunctional perovskite catalyst for oxygen reduction and evolution. Angew Chem. 2014;126(18):4670–4.
[109] Jung JI, Risch M, Park S, Kim MG, Nam G, Jeong HY, et al. Optimizing nanoparticle perovskite for bifunctional oxygen electrocatalysis. Energy Env Sci. 2016;9(1):176–83.
[110] Hjalmarsson P, Søgaard M, Mogensen M. Electrochemical performance and degradation of $(La_{0.6}Sr_{0.4})_{0.99}CoO_{3-\delta}$ as porous SOFC-cathode. Solid State Ion. 2008;179(27–32):1422–6.
[111] Chen Z, Yu A, Higgins D, Li H, Wang H, Chen Z. Highly active and durable core-corona structured bifunctional catalyst for rechargeable metal-air battery application. Nano Lett. 2012;12(4):1946–52.
[112] Chen S, Duan J, Jaroniec M, Qiao SZ. Nitrogen and oxygen dual-doped carbon hydrogel film as a substrate-free electrode for highly efficient oxygen evolution reaction. Adv Mater. 2014;26(18):2925–30.
[113] Yu X, Zhang M, Chen J, Li Y, Shi G. Nitrogen and sulfur codoped graphite foam as a self-supported metal-free electrocatalytic electrode for water oxidation. Adv Energy Mater. 2016;6(2):1–9.
[114] Wang S, Zhang L, Xia Z, Roy A, Chang DW, Baek JB, et al. BCN graphene as efficient metal-free electrocatalyst for the oxygen reduction reaction. Angew Chem - Int Ed. 2012;51(17):4209–12.
[115] Yang L, Jiang S, Zhao Y, Zhu L, Chen S, Wang X, et al. Boron-doped carbon nanotubes as metal-free electrocatalysts for the oxygen reduction reaction. Angew Chem - Int Ed. 2011;50(31):7132–5.
[116] Wang S, Iyyamperumal E, Roy A, Xue Y, Yu D, Dai L. Vertically aligned BCN nanotubes as efficient metal-free electrocatalysts for the oxygen reduction reaction: a synergetic effect by

co-doping with boron and nitrogen. Angew Chem - Int Ed. 2011;50(49):11756–60.
[117] Qu L, Liu Y, Baek JB, Dai L. Nitrogen-doped graphene as efficient metal-free electrocatalyst for oxygen reduction in fuel cells. ACS Nano. 2010;4(3):1321–6.
[118] Tian GL, Zhang Q, Zhang B, Jin YG, Huang JQ, Su DS, et al. Toward full exposure of "active sites": nanocarbon electrocatalyst with surface enriched nitrogen for superior oxygen reduction and evolution reactivity. Adv Funct Mater. 2014;24(38):5956–61.
[119] Zhang J, Zhao Z, Xia Z, Dai L. A metal-free bifunctional electrocatalyst for oxygen reduction and oxygen evolution reactions. Nat Nanotechnol. 2015;10(5):444–52.
[120] Ma TY, Ran J, Dai S, Jaroniec M, Qiao SZ. Phosphorus-doped graphitic carbon nitrides grown *in situ* on carbon-fiber paper: flexible and reversible oxygen electrodes. Angew Chem. 2015;127(15):4729–33.
[121] Park J, Kim J, Yang Y, Yoon D, Baik H, Haam S, et al. RhCu 3D nanoframe as a highly active electrocatalyst for oxygen evolution reaction under alkaline condition. Adv Sci. 2016;3(4):1–8.
[122] An L, Huang L, Zhou P, Yin J, Liu H, Xi P. A self-standing high-performance hydrogen evolution electrode with nanostructured $NiCo_2O_4$/CuS heterostructures. Adv Funct Mater. 2015;25(43):6814–22.
[123] Xu W, Lu Z, Wan P, Kuang Y, Sun X. High-performance water electrolysis system with double nanostructured superaerophobic electrodes. Small. 2016;12(18):2492–8.
[124] Zhang X, Xu H, Li X, Li Y, Yang T, Liang Y. Facile synthesis of nickel-iron/nanocarbon hybrids as advanced electrocatalysts for efficient water splitting. ACS Catal. 2016;6(2):580–8.
[125] Ma J, Wei H, Liu Y, Ren X, Li Y, Wang F, et al. Application of Co_3O_4-based materials in electrocatalytic hydrogen evolution reaction: a review. Int J Hydrog Energy. 2020;45(41):21205–20.
[126] Yan Y, Xia BY, Ge X, Liu Z, Fisher A, Wang X. A flexible electrode based on iron phosphide nanotubes for overall water splitting. Chem-A Eur J. 2015;21(50):18062–7.
[127] Li X, Zhang R, Luo Y, Liu Q, Lu S, Chen G, et al. A cobalt-phosphorus nanoparticle decorated N-doped carbon nanosheet array for efficient and durable hydrogen evolution at alkaline pH. Sustain Energy Fuels. 2020;4(8):3884–7.
[128] Wang J, Cui W, Liu Q, Xing Z, Asiri AM, Sun X. Recent progress in cobalt-based heterogeneous catalysts for electrochemical water splitting. Adv Mater. 2016;28(2):215–30.
[129] Du S, Ren Z, Zhang J, Wu J, Xi W, Zhu J, et al. Co_3O_4 nanocrystal ink printed on carbon fiber paper as a large-area electrode for electrochemical water splitting. Chem Commun. 2015;51(38):8066–9.
[130] Wang H, Lee HW, Deng Y, Lu Z, Hsu PC, Liu Y, et al. Bifunctional non-noble metal oxide nanoparticle electrocatalysts through lithium-induced conversion for overall water splitting. Nat Commun. 2015;6:7261.
[131] Jin H, Wang J, Su D, Wei Z, Pang Z, Wang Y. In situ cobalt-cobalt oxide/N-doped carbon hybrids as superior bifunctional electrocatalysts for hydrogen and oxygen evolution. J Am Chem Soc. 2015;137(7):2688–94.
[132] Li J, Wang Y, Zhou T, Zhang H, Sun X, Tang J, et al. Nanoparticle superlattices as efficient bifunctional electrocatalysts for water splitting. J Am Chem Soc. 2015;137(45):14305–12.
[133] Xu S, Zhao H, Li T, Liang J, Lu S, Chen G, et al. Iron-based phosphides as electrocatalysts for the hydrogen evolution reaction: recent advances and future prospects. J Mater Chem A. 2020;8(38):19729–45.
[134] Chen GF, Ma TY, Liu ZQ, Li N, Su YZ, Davey K, et al. Efficient and stable bifunctional electrocatalysts Ni/NixMy (M = P, S) for overall water splitting. Adv Funct Mater. 2016;26(19):3314–23.
[135] You B, Jiang N, Sheng M, Gul S, Yano J, Sun Y. High-performance overall water splitting electrocatalysts derived from cobalt-based metal-organic frameworks. Chem Mater. 2015;27(22):7636–42.
[136] Xu J, Gao J, Wang C, Yang Y, Wang L. NH_2-MIL-125(Ti)/graphitic carbon nitride heterostructure decorated with NiPd cocatalysts for efficient photocatalytic hydrogen production. Appl Catal B Env. 2017;219:101–8.
[137] Ventrapragada LK, Creager SE, Rao AM, Podila R. Carbon nanotubes coated paper as current collectors for secondary li-ion batteries. Nanotechnol Rev. 2019;8(1):18–23.
[138] Visconti P, Primiceri P, Fazio Rde, Strafella L, Ficarella A, Carlucci AP. Light-Induced ignition of carbon nanotubes and energetic nano-materials: a review on methods and advanced technical solutions for nanoparticles-enriched fuels combustion. Rev Adv Mater Sci. 2020;59(1):26–46.
[139] Ito Y, Cong W, Fujita T, Tang Z, Chen M. High catalytic activity of nitrogen and sulfur co-doped nanoporous graphene in the hydrogen evolution reaction. Angew Chemie. 2015;127(7):2159–64.
[140] Barathi Dassan EG, Rahman AAAb, Abidin MSZ, Akil HMd. Carbon nanotube-reinforced polymer composite for electromagnetic interference application: a review. Nanotechnol Rev. 2020;9(1):768–88.
[141] Lin Z, Waller GH, Liu Y, Liu M, Wong CP. Simple preparation of nanoporous few-layer nitrogen-doped graphene for use as an efficient electrocatalyst for oxygen reduction and oxygen evolution reactions. Carbon N Y. 2013;53:130–6.
[142] Zhang J, Xia Z, Dai L. Carbon-based electrocatalysts for advanced energy conversion and storage. Sci Adv. 2015;1(7):e1500564.
[143] Ma TY, Dai S, Qiao SZ. Self-supported electrocatalysts for advanced energy conversion processes. Mater Today. 2016;19(5):265–73.
[144] Duan J, Chen S, Jaroniec M, Qiao SZ. Heteroatom-doped graphene-based materials for energy-relevant electrocatalytic processes. ACS Catal. 2015;5(9):5207–34.
[145] Zeng M, Li Y. Recent advances in heterogeneous electrocatalysts for the hydrogen evolution reaction. J Mater Chem A. 2015;3(29):14942–62.
[146] Zhao Y, Nakamura R, Kamiya K, Nakanishi S, Hashimoto K. Nitrogen-doped carbon nanomaterials as non-metal electrocatalysts for water oxidation. Nat Commun. 2013;4:2–8.
[147] Zheng Y, Jiao Y, Li LH, Xing T, Chen Y, Jaroniec M, et al. Toward design of synergistically active carbon-based catalysts for electrocatalytic hydrogen evolution. ACS Nano. 2014;8(5):5290–6.
[148] Lai J, Li S, Wu F, Saqib M, Luque R, Xu G. Unprecedented metal-free 3D porous carbonaceous electrodes for full water splitting. Energy Environ Sci. 2016;9(4):1210–4.

[149] Xu S, Lei Z, Wu P. Facile preparation of 3D MoS_2/$MoSe_2$ nanosheet-graphene networks as efficient electrocatalysts for the hydrogen evolution reaction. J Mater Chem A. 2015;3(31):16337–47.
[150] Dou S, Tao L, Huo J, Wang S, Dai L. Etched and doped Co_9S_8/graphene hybrid for oxygen electrocatalysis. Energy Environ Sci. 2016;9(4):1320–6.
[151] Wang DY, Gong M, Chou HL, Pan CJ, Chen HA, Wu Y, et al. Highly active and stable hybrid catalyst of cobalt-doped FeS_2 nanosheets-carbon nanotubes for hydrogen evolution reaction. J Am Chem Soc. 2015;137(4):1587–92.
[152] Tang C, Cheng N, Pu Z, Xing W, Sun X. NiSe nanowire film supported on nickel foam: an efficient and stable 3D bifunctional electrode for full water splitting. Angew Chemie. 2015;127(32):9483–7.
[153] Shi J, Hu J, Luo Y, Sun X, Asiri AM. Ni_3Se_2 film as a non-precious metal bifunctional electrocatalyst for efficient water splitting. Catal Sci Technol. 2015;5(11):4954–8.
[154] Lu Z, Zhu W, Yu X, Zhang H, Li Y, Sun X, et al. Ultrahigh hydrogen evolution performance of under-water "superaerophobic" MoS_2 nanostructured electrodes. Adv Mater. 2014;26(17):2683–7.
[155] Han J, Wang D, Zhang P. Effect of nano and micro conductive materials on conductive properties of carbon fiber reinforced concrete. Nanotechnol Rev. 2020;9(1):445–54.
[156] Hou CC, Cao S, Fu WF, Chen Y. Ultrafine CoP nanoparticles supported on carbon nanotubes as highly active electrocatalyst for both oxygen and hydrogen evolution in basic media. ACS Appl Mater Interfaces. 2015;7(51):28412–9.
[157] Jiang N, You B, Sheng M, Sun Y. Electrodeposited cobalt-phosphorous-derived films as competent bifunctional catalysts for overall water splitting. Angew Chemie. 2015;127(21):6349–52.
[158] Ledendecker M, Krickcalderõn S, Papp C, Steinrück HP, Antonietti M, Shalom M. The synthesis of nanostructured Ni_5P_4 films and their use as a non-noble bifunctional electrocatalyst for full water splitting. Angew Chemie - Int Ed. 2015;54(42):12361–5.
[159] Jiao L, Zhou YX, Jiang HL. Metal-organic framework-based CoP/reduced graphene oxide: high-performance bifunctional electrocatalyst for overall water splitting. Chem Sci. 2016;7(3):1690–5.
[160] Feng LL, Yu G, Wu Y, Li GD, Li H, Sun Y, et al. High-index faceted ni_3s_2 nanosheet arrays as highly active and ultrastable electrocatalysts for water splitting. J Am Chem Soc. 2015;137(44):14023–6.
[161] Hou Y, Lohe MR, Zhang J, Liu S, Zhuang X, Feng X. Vertically oriented cobalt selenide/NiFe layered-double-hydroxide nanosheets supported on exfoliated graphene foil: an efficient 3D electrode for overall water splitting. Energy Environ Sci. 2016;9(2):478–83.
[162] Zhu H, Zhang J, Yanzhang R, Du M, Wang Q, Gao G, et al. When cubic cobalt sulfide meets layered molybdenum disulfide: a core-shell system toward synergetic electrocatalytic water splitting. Adv Mater. 2015;27(32):4752–9.
[163] Jahan M, Liu Z, Loh KP. A graphene oxide and copper-centered metal organic framework composite as a tri-functional catalyst for HER, OER, and ORR. Adv Funct Mater. 2013;23(43):5363–72.
[164] Hou Y, Wen Z, Cui S, Ci S, Mao S, Chen J. An advanced nitrogen-doped graphene/cobalt-embedded porous carbon polyhedron hybrid for efficient catalysis of oxygen reduction and water splitting. Adv Funct Mater. 2015;25(6):872–82.
[165] Liu X, Liu W, Ko M, Park M, Kim MG, Oh P, et al. Metal (Ni, Co)-metal oxides/graphene nanocomposites as multifunctional electrocatalysts. Adv Funct Mater. 2015;25(36):5799–808.
[166] Jiang H, Gu J, Zheng X, Liu M, Qiu X, Wang L, et al. Defect-rich and ultrathin N doped carbon nanosheets as advanced trifunctional metal-free electrocatalysts for the ORR, OER and HER. Energy Environ Sci. 2019;12(1):322–33.
[167] Li M, Zhang L, Xu Q, Niu J, Xia Z. N-doped graphene as catalysts for oxygen reduction and oxygen evolution reactions: theoretical considerations. J Catal. 2014;314:66–72.
[168] Zhao Z, Li M, Zhang L, Dai L, Xia Z. Design principles for heteroatom-doped carbon nanomaterials as highly efficient catalysts for fuel cells and metal-air batteries. Adv Mater. 2015;27(43):6834–40.